

Please cite the Published Version

Omran, BA, Whitehead, KA and Baek, KH (2021) One-pot bioinspired synthesis of fluorescent metal chalcogenide and carbon quantum dots: Applications and potential biotoxicity. Colloids and Surfaces B: Biointerfaces, 200. ISSN 0927-7765

DOI: <https://doi.org/10.1016/j.colsurfb.2021.111578>

Publisher: Elsevier

Version: Accepted Version

Downloaded from: <https://e-space.mmu.ac.uk/627260/>

Usage rights: © In Copyright

Additional Information: This is an Author Accepted Manuscript of an article published in Colloids and Surfaces B: Biointerfaces.

Enquiries:

If you have questions about this document, contact openresearch@mmu.ac.uk. Please include the URL of the record in e-space. If you believe that your, or a third party's rights have been compromised through this document please see our Take Down policy (available from <https://www.mmu.ac.uk/library/using-the-library/policies-and-guidelines>)

One-pot bioinspired synthesis of fluorescent metal chalcogenide and carbon quantum dots: Applications and potential biotoxicity

Basma A. Omran ^{a,b}, Kathryn A. Whitehead ^c, and Kwang-Hyun Baek ^{a,*}

^a Department of Biotechnology, Yeungnam University, Gyeongsan 38541, Republic of Korea, obasma@ynu.ac.kr

^b Department of Processes Design & Development, Egyptian Petroleum Research Institute (EPRI), Nasr City 11727, Cairo, Egypt

^c Microbiology at Interfaces, Manchester Metropolitan University, Chester Street, Manchester M1 5GD, United Kingdom, k.a.whitehead@mmu.ac.uk

* Correspondence: khbaek@ynu.ac.kr; Tel.: +82-53-810-3029; Fax: +82-53-810-4769.

Abstract

Quantum dots (QDs) are promising nanoscale materials with sizes ranging from 1 to 10 nm, and have exponentially triggered scientific interest worldwide during the past decade. They exhibit size-tunable optical features, zero-dimensional structures, and quantum confinement effects. Moreover, they can be tailored to suit various applications. Phyto-synthesis of fluorescent metal chalcogenide QDs and carbon dots (CDs) is a green, feasible, low-cost, and environmentally safe approach to overcome the limitations of chemical and physical synthesis techniques. Different plant extracts provide several phytochemical constituents with numerous functional moieties for natural capping and stabilization of the synthesized metal chalcogenide QDs and CDs. Therefore, the green synthesis of metal chalcogenide QDs and CDs, their optical and structural properties, and applications such as diagnostics, biosensing, heavy metal detection, and photocatalytic degradation are comprehensively summarized in this review. Furthermore, the biovalorization of agricultural wastes, such as fruit and vegetable peels, is addressed to produce high-value metal chalcogenide QDs and CDs. In addition, the toxicity issues associated with these particles are described for the safe usage of QDs. Challenges that restrict the widespread application of QD particles are discussed along with future perspectives for their commercial, safe, and upscale production.

Keywords: Green synthesis, Plant extracts, Waste biovalorization, Applications, Biotoxicity.

1. Introduction

Nanotechnology is a state-of-the-art science that deals with nanosized structures (1–100 nm). The implementation of nanomaterials has gained immense attention worldwide [1]. Quantum dots (QDs) are a class of nanoparticles and are considered as the newest generation of nanosized materials with a size range of 1–10 nm [2, 3]. The QD term originated from the fact that QDs exhibit properties of nanocrystals, which are dominated by quantum theories and mechanics [4], that is, QDs are characterized by outstanding properties such as high photostability with high volume to surface ratio, high quantum yield (QY), large Stokes shift, and resistance to photobleaching [5, 6]. From a structural point of view, QDs comprise a semiconductor core, overlaid with a shell capped with ligands to improve their solubility in aqueous media [7]. In general, QDs are made up of combinations of metal and transition elements, belonging to III–V, II–VI, and IV–VI groups [8]. QDs are presently being assessed in a wide range of applications, e.g., disease diagnosis, bioimaging, tissue engineering, drug delivery, microbial labeling, biosensing, single protein

tracking and therapy, photothermal therapy, and tumor research, etc. [9, 10]; however, their application is still in its infancy.

The pioneering breakthroughs in nanotechnology over the past few decades facilitated the preparation, processing, architecture, and assembly of nanosized materials using top-down and bottom-up approaches. Typically, the chemical synthesis strategies are complicated due to their high costs and slow reaction, in addition to the reduced yields [11]. Moreover, noxious chemicals such as sodium borohydride and dimethyl formamide are usually employed; however, they lead to various hazards and risks [12]. Green chemistry approaches emerged in the mid-1990s and dealt with the issues such as avoidance and prevention of hazardous chemicals, longevity, maximization of performance, and conservation [13]. Biological fabrication is an innovative and developing platform of the present century that has the potential to dramatically change the fate of applications of nanomaterials in various disciplines [14]. The integration of nanotechnology with plants and their byproducts is referred to as “phytonanotechnology” [15]. Considering the recent trend toward sustainability, phytonanotechnology is gaining immense interest nowadays due to its potential to convert metals into their nanoparticle state by using extracts of several plant parts, including roots, seeds, stems, shoots, gum, and leaves, in addition to fruit and vegetable waste byproducts [12]. In general, fresh and healthy plant parts are selected and washed thoroughly to remove any surface contaminants. Water is the main solvent used to prepare the plant extracts.

Food sustainability, as discussed by the Sustainable Development of the United Nations, is the main concern, which has grabbed the attention of international organizations [16]. Agricultural production and excellent control of food supplies are crucial parameters to guarantee food security, as in 2100, the human population worldwide is expected to exceed 12.3 billion [17]. Moreover, an immense amount of food waste is produced annually, that is, approximately 1.3 billion tons are lost each year according to the Food and Agricultural Organization [16]. Consequently, sustainability is not just implied to particular agricultural practices, but also to the management of the elevated levels of agricultural waste being generated. Usually, waste monitoring protocols involve treatment, minimization, and elimination techniques to reduce the devastating influence of wastes on the surrounding ecosystem. Conventional disposal strategies involve landfilling and incineration; however, these strategies have certain limitations as they are lethal to humans and the surrounding biota [18]. Hence, the demand for better and eco-friendly strategies has gained interest of researchers worldwide. Waste biovalorization to more valuable and beneficial products has become the need of the hour. These products may include nanomaterials, pharmaceuticals, chemicals, fuel, and biomaterials, and others. The abundance of several phytochemical constituents in plants and agricultural wastes (e.g., peels of fruits and vegetables) facilitates the synthesis of nanomaterials and provides natural stabilizers and capping agents [19]. Thus, the use of agricultural wastes and plant extracts is receiving considerable attention from the modern society [20].

Several studies have discussed the possible use of extracts of plants and agricultural wastes as potential mediators for the green synthesis of QDs [1, 9, 21]. Therefore, the following sections emphasize the phyto-synthesis of metal chalcogenide QDs and carbon dots (CDs) by using extracts of different plant parts and agricultural wastes as the present phytochemical constituents play a crucial role in mediating the synthesis of QDs. Furthermore, the properties

and diverse applications of green-synthesized metal QDs and CDs along with toxicity issues are discussed by addressing their biosafety using numerous cell lines and animal models.

2. Green synthesis of QDs, advantages, and disadvantages

In the famous words of Albert Einstein, "*We're going to need a significantly different way of thinking for humanity to be able to survive*" [22]. The rapid industrial developments represented a cornerstone for the worldwide economic advance. Even though industrialization contributed enormously to improve the quality of human daily life, worldwide policies remained unconscious of the consequences of industrial growth and its impact on the environment and the planet. Environmental problems have started to arise since the 1940s as a result of the massive and rapid increase in industrial activities [23]. Coping with the global environmental risks and problems, several conferences and political decisions have emphasized the urgent need for adopting a sustainable, clean, and eco-friendly framework for the synthesis of new products. In 1949, the initial concerns regarding the industrial impacts on the environment started at the United Nations Conference on Conservation and Use of Resources in the USA. Then, environmental concerns attracted more attention in 1968 at the Biosphere Conference [24]. Then, during the 1960s, the book "Silent Spring" was published and the historical book contributed to raising environmental awareness in regards to the risks associated with excessive use of natural resources [25].

The concept "Green Chemistry", which was offered to the scientific world in 1991, was meant to minimize or eliminate the use of toxic materials and to reduce human and environmental exposure to chemicals. The twelve key principles of green chemistry were released in the 1990s by John Warner and Paul Anastas, and they are still in use today [24]. These principles encompassed the need to minimize or exclude the use of harmful solvents throughout the chemical processes. The principles highlighted the importance of the absolute no generation of any toxic discharges or wastes from chemical processes [26]. Additionally, the principles proposed the importance of applying eco-friendly guidance during the synthesis, processing, and analysis of any chemical product. The main target of these principles was to reduce any inherent occupational or environmental hazards during industrial activities [27].

QDs represent the nano-age ball bearings and a key driving force behind the modern industrial nano revolution because of their high photostability and intense luminescence [28]. Major improvements in manufacturing QDs would be required to achieve their promising applications [29]. QDs are usually prepared via top-down and bottom-up approaches. In top-down approaches, QDs are synthesized by thinning the bulk semiconductor or carbon material to obtain small-sized particles [30]. The top-down methodologies include high-energy laser, reactive-ion etching, electron beam lithography, chemical oxidation, and plasma etching [31]. On the other hand, QD bottom-up synthesis depends on generating QDs by self-assembling, ordering, and arraying of atoms via supramolecular electrostatic, π - π , hydrophilic and hydrophobic interactions, Van der Waals forces, and hydrogen bonding [32]. Bottom-up approaches include wet-chemical methods such as microwave- and ultrasound-assisted techniques, sol-gel, hot-solution decomposition, hydrothermal, and green/biological synthesis [33]. However, the chemical and physical synthesis techniques retain impurities in the produced QDs, which lead to structural imperfections in addition to the disadvantages related to high expenses [34]. The financial aspects have a key role to play in transmitting technology expertise from research centers to industries, markets, and consumers. The chemical synthesis of QDs depends on using several organophosphorus solvents whose price can account for up to 90% of the total production costs.

Accordingly, the choice of the solvents as reductants such as hydrazine hydrate and sodium borohydride is an important issue affecting the accumulative impact of the chemical synthesis because of the toxic effects on humans and the surrounding ecosystem [35]. This has necessitated more investigations into biological methodologies as they are facile, green, and environmentally friendly.

In line with the main principles of green chemistry, nanobiotechnology arose as an effective biological route for nanoparticle synthesis which can employ sustainable approaches. Different biological entities have mediated the synthesis of QDs including; bacteria [36, 37], yeast [38, 39], fungi [40, 41], algae [42, 43], and extracts of different plant parts [44, 45] and agro-industrial wastes [46]. The field of phytonanotechnology is multidisciplinary and medically relevant [17]. Green synthesis of QDs possesses several distinctive advantages when compared with the chemical and physical synthesis techniques. The synthesized particles are further stabilized by the bioactive molecules such as carbohydrates, proteins, and other organic constituents [47]. Additionally, enzymes within the biological nanofactories play a crucial role in binding to metal ions and subsequent reduction to nanoscale-sized particles [48]. This takes place with the aid of several functional moieties such as hydroxyl, carboxyl, sulfhydryl, and amino groups. Numerous studies have potentially reported the use of water as a sole solvent during the production of QDs using the plants' and agro-industrial waste extracts [49-52]. Green synthesis of QDs is economically feasible, energy and time saving, and environmentally friendly because there is no need for the hazardous and expensive chemical solvents which can result in serious environmental problems [53]. In comparison with the conventional chemical and physical techniques, QD green synthesis is carried out at neutral pH and almost ambient temperature. Other advantages involve; enhanced stability, scaling-up, sustainability, and biocompatibility.

The terms "circular economy or bioeconomy" have been coined by the European Commission in 2012 as "the parts of the economy which are mainly dependent on the use of renewable and sustainable biological resources to produce food, energy, and materials" [22]. The idea of the circular economy is based on waste minimization, resource conservation, regeneration, recycling, and transformation of biological resources into commercially sustainable materials and bioenergy. Agro-industrial and food wastes are key targets of the circular economy which can be turned into high-value-added products [54]. These wastes show pH variations and different compositions with high chemical and biological oxygen demands. The high water and nutritional contents provide excellent breeding habitats for disease-causing pathogens which lead to microbial contamination, which in turn postures serious environmental issues [55]. Nevertheless, the presence of untreated agricultural and food wastes for long terms in landfill sites has ended up with the generation of high levels of methane, which is a greenhouse gas and it is more detrimental than carbon dioxide. It is considered a contributing factor to global warming and climate change [56].

Established practical strategies applied in agricultural and food sectors are unable to resolve such waste management problems [57]. Consequently, this problem requires the implementation of resource management systems with sustainable aspects for the valorization of agricultural and food wastes [58]. For instance, *Citrus* fruits are considered the most utilized fruits in the world due to their high nutritional benefits and high content of secondary metabolites. Only one-third of the *Citrus* fruits are used for processing, hence this leads to the generation of 50-60% organic wastes [59]. The management of solid residual *Citrus* wastes remains the main concern for *Citrus* processing industries. The solid wastes which are remained after juice extraction procedures are usually made up of peels, seeds,

membranes, rags, and leaf residues [60]. Traditional management strategies involve landfilling and incineration, which are currently provoked as problematic strategies in regards to the environmental impacts [61]. In this context, several reports have demonstrated the efficiency of valorizing *Citrus* wastes for the green synthesis of biosorbents [62, 63], biofertilizers [64], biofuels [65, 66], nanomaterials [67, 68], and QDs [69, 70]. Agricultural and food waste valorization will provide greater protection to the environment through the elimination of such waste and by mediating the synthesis of valuable products such as QDs.

Nevertheless, certain disadvantages of green fabrication of QDs require deep investigations to resolve. The most prominent drawbacks of plant-assisted green synthesis are the difficulties in the complete separation of QDs from the biomass. However, the need for additional separation steps could lead to a negative interference mostly on potential pilot scales or major manufacturing of green synthesized particles [71]. Standardization of QD green fabrication is difficult since QD fluorescent properties and quantum yields are correlated with the chemical functionalities present on the QD surface. Effective green synthesis of QDs must optimize the different parameters which would affect the preparation of specific size, shape, and monodispersed particles [47]. These factors involve reaction time, metal salt and substrate concentrations, pH, temperature, etc. For a thorough understanding of the QD green synthesis, the biochemical components involved in the reduction of metal salts have to be isolated and identified [72]. However, the presence of various forms of phytochemicals makes it a challenging task. Furthermore, the difficulty in assessing the precise chemical configuration of the biological capping and stabilizing molecules necessitates more investigations. The industrial upscaling of QDs needs to be more operational and this can be attained by applying facile, green, and cost-effective techniques and by optimizing the synthesis conditions [73]. The implementation of synthetic approaches focused on the use of renewable precursor materials is quite insightful and demands further comprehensive studies for commercial and industrial scales [74]. Most notably, one of the continuing challenges is to boost and develop the quantum yield of QDs while making full use of their inherent characteristics and fine-tuning their strong fluorescence emission spectra particularly for biomedical applications [75]. Controlling the green synthesis tactics, degree of crystallinity, surface morphology, nano-scale impact, and conceptual size are challenging issues as they are tightly correlated to the luminescence phenomenon, which needs careful handling, accurate synthesis, and critical analysis [76].

Overall, the summary of several studies indicates that researchers are searching for novel, cost-effective, and sustainable raw materials and techniques that can be implemented for QD green synthesis at mild conditions based on green chemistry conceptual knowledge. The on-going promising collaboration between several disciplines involving biotechnology, physics, photonics, engineering, nanomedicine, toxicology, and other scientific fields will make QD green synthesis reaches a milestone in this global nano-revolution.

3. Structural and optical properties and versatile applications of phyto-synthesized metal chalcogenide QDs

Transitional metals such as lead, cadmium, manganese, and zinc can produce chalcogenide molecules or chalcogens via conjugation with selenides, oxides, tellurides, and sulfides [77]. Chalcogens have received remarkable attention and have been extensively studied due to their narrow emission and absorption spectra, size-dependent emissions, and excellent optical and catalytic features [78]. The different classes of QDs, characteristic features (e.g. energy band gap, quantum yield, absorption band, absorption and emission ranges and confinement of excited electron

184 and holes) in addition to the limitations of each class are described in Table (1). Chalcogens have a myriad of
185 applications involving chemical industry, environmental remediation, and energy transformation [79]. The implication
186 of green synthesis has markedly increased as it aids in reducing power consumption and generating minimal hazardous
187 waste.

188

Table 1

189

Different classes of metal chalcogenide QDs, characteristics, limitations, and examples of construction materials (core/shell).

Types of QDs	Energy band gap (EBG)	Confinement of excited electron and holes	Stokes Shift	Quantum Yield (QY)	Absorption range (nm)	Emission range (nm)	Drawbacks	Examples of construction materials (core/shell)	References
Type I	The EBG of the shell material is larger than that of the core material	Excited electron and holes are confined to the core region as both the valence and the conduction band edges are located within the EGB of the shell	Small	High and long term stable QY	400-500	430-600	Reduced fluorescence owing to trapping carrier charges	CdSe/ CdS, CdSe/ZnS, CdTe/CdS and CdSe/ InAs	[80]
Inverse Type I	The EBG of the shell material is narrower than that of the core material	Excited electron and holes are partially delocalized to the shell region	Relatively large	Low and poor term stable QY	400-500	400-700	Leakage of excited electrons and holes to the surface of nanocrystal	CdS/HgS, CdS/CdSe, ZnS/CdSe and ZnSe/CdSe	[81]
Type II	The EBG of the core material is narrower than that of the shell material	One excited electron or hole is confined to the core whilst the other is confined to the shell	Large	Low and poor term stable QY	600-800	700-1000	Leakage of excited electrons and holes to the surface of nanocrystal	CdTe/CdSe, CdTe/CdSe, and ZnTe/ ZnSe	[82]
Inverse Type II	The EBG of the core material is larger than that of the shell material	One excited electron or hole is confined to the shell whilst the other is confined within the core	Large and tunable by controlling shell thickness and core size	Relatively high and stable QY	300-1600	700-1000	Reduction in excited decay time due to excited electrons or holes	Inp/CdS and PbS/CdS	[83]

190

3.1. Metal chalcogenide QDs derived from the extracts of different plant parts

Cadmium sulfide QDs (CdS QDs) have been synthesized via an eco-friendly route using castor oil (CSTO) and ricinoleic acid (a CSTO derivative) [84]. CSTO was obtained from the seed extract of *Ricinus communis*. CSTO and its derivatives are natural organic surfactants, and they act as bio-based capping agents during the synthesis of CdS QDs. UV/Vis spectroscopy of the CSTO-mediated CdS QDs revealed typical absorption peak characteristic of CdS. The influence of three temperatures on the synthesis of CSTO-derived CdS QDs (230°C, 250°C, and 280°C) was tested. Samples prepared at 250°C and 280°C exhibited sharper absorbance peaks than those synthesized at lower temperatures. Similar observations were recorded for the ricinoleic-acid-capped CdS QDs. CSTO and ricinoleic acid-derived CdS QDs were almost spherical in shape and their sizes were 4.64 ± 0.35 and 5.60 ± 0.92 nm, respectively. Energy dispersive X-ray (EDX) analysis presented a clear elemental composition of the CdS particles. Fourier-transform infrared (FTIR) spectra confirmed that the CdS QDs were successfully capped by ricinoleic acid and CSTO. The indexing of the X-ray diffraction (XRD) peaks was in accordance with the hexagonal crystalline reflections of CdS.

The biosynthesis of tin oxide QDs (SnO₂ QDs) using an aqueous pod extract of stinky beans (*Parkia speciosa* Hassk.) was reported [50]. A characteristic UV/Vis absorption peak of the SnO₂ QDs appeared at 270 nm. The band energy gap (BEG) was 4.17 eV. The diffraction peaks in the XRD patterns were in accordance with those of the tetragonal standard SnO₂ with high purity. The average crystallite size calculated using the Debye–Scherer equation was estimated to be 1.5 nm. The prepared SnO₂ particles were in the quantum-confinement regime. This was confirmed by the average size of the prepared particles, which was lower than the SnO₂ Bohr’s radius, hence confirming their high quantum-confinement effect. FTIR identified the presence of several bridging bonds denoted by the vibrational stretching of Sn–O and O–Sn–O. Moreover, hydroxyl functional groups were detected, which might be ascribed to the antioxidant constituents. These components might have been absorbed on the surface of the synthesized particles through π -electron linkages. Two elemental signals appeared at 0.5 and 3.4 Kev, corresponding to oxygen and tin, respectively. The prepared particles displayed a rounded morphological structure, as illustrated by transmission electron microscope (TEM), with an approximate diameter of 1.9 nm. The lattice fringes were further identified via a high-resolution (HR) TEM and were found to be 0.17 and 0.26, thereby corresponding to the SnO₂ planes 211 and 101, respectively. The prepared SnO₂ QD particles displayed excellent photocatalytic potential for the degradation of the acid yellow 23 dye under UV light. The maximum photodegradation activity of the SnO₂ QD particles reached 98% and was attained within 24 h of reaction time using 25 mg of SnO₂ QDs and 5 mg/L of the tested dye. Interestingly, the biosynthesized catalyst could be reused for five successive cycles without affecting its proficiency or stability. Furthermore, the biosynthesized SnO₂ QDs exhibited high antioxidant activity, with an IC₅₀ value of 312.6 ± 0.025 μ g/mL. *Thevetia peruviana* is an ornamental plant species native to Central and Southern America and is found in the tropical and temperate areas. The leaf extract of *T. peruviana* contains flavonols, phenols, glycosides, and proteins.

Cadmium telluride QDs (CdTe QDs) with a size of 4–6 nm were prepared using *T. peruviana* leaf extract [85]. An aqueous extract of *Ficus johannis* mediated the green synthesis of CdTe QDs [86]. Microwave extraction (90 and 270 w for 15 min) and ultrasonic-assisted extraction (at 45°C for 15 min) processes were applied for the preparation

of *F. johnnis* extract. The mean particle size was estimated as 1.2 nm. The prepared CdTe QDs expressed an antimicrobial potential against Gram-positive (*Staphylococcus aureus* and *Bacillus subtilis*) and Gram-negative (*Escherichia coli* and *Pseudomonas aeruginosa*) and an antifungal activity against *Candida albicans* and *Aspergillus oryzae*. Interestingly, the CdTe QDs prepared at the high microwave irradiation power (i.e. 270 w) displayed a more antibacterial effect compared with the other samples prepared at 90 w and by the ultra-sonic assisted procedure. Additionally, the *F. johnnis* derived CdTe QDs possessed an antioxidant potential.

Generation of reactive oxygen species (ROS) (e.g. $O_2^{\cdot-}$, H_2O_2 , and OH^{\cdot}) and initiation of oxidative stress are the key toxicological mechanisms by which metal chalcogenide QDs can damage bacterial cells [87]. Hydroxyl radicals are more reactive than the other free radicals and they can lead to disruption of bacterial electron transport chain and initiation of mutations [88]. Free radicals cause lipid oxidation, protein denaturation, and nucleic acid modification. Metal chalcogenide QDs dissociate and form metal ions (e.g. Cd ions) and the free orbitals of the resultant ions (e.g. Cd^{+2}) interact with the free electron pairs present in nitrogen and oxygen atoms in bacterial cells and form chelate, which inactivates bacterial components [89].

The antibacterial action of metal chalcogenides is affected by parameters such as the difference in the bacterial cell wall structure of both Gram classes, size of the metal chalcogenide QDs, and degree of interaction between bacteria and the particles [90]. Khezripour et al. [91] reported that the antibacterial action of ZnSe QDs against *E. coli*, *S. aureus*, *P. aeruginosa*, and *B. cereus* was due to their small size (~2 nm). *E. coli* and *P. aeruginosa* were more sensitive to ZnSe QDs than *B. cereus* and *S. aureus*. Similar observations were recorded by Ali et al. [92] and Chaliha et al. [93]. Gram-positive bacteria possess a thick cell wall with linear complex chains of polysaccharides, which make their penetration difficult, while the thickness of the cell wall of Gram-negative bacteria is less, which in turn allows the penetration of QDs [94]. However, this was contradictory with the study performed by Baruah et al. [95] in which the antibacterial action of ZnS QDs was assessed against *S. aureus* and *P. aeruginosa*. Results showed that despite having a thicker peptidoglycan layer, Gram-positive bacteria showed more sensitivity toward ZnS QDs compared to Gram-negative bacteria; which might be attributed to the absence of an outer cell membrane. Additionally, the antibacterial potential was attributed to the very small size (i.e. 5 nm). It is known that the smaller the size of the nanoparticles, the greater their diffusion potency, and the easier their penetration through the cell membrane pores [96].

Semiconductor CdS QDs possess exceptional biological and medical applications, such as cell labeling, disease diagnosis, and imaging of intercellular processes. The efficiency of radish (*Rhaphanus sativus* L.) hairy roots was assessed to synthesize CdS QDs [97]. Sharp absorbance and emission peaks were observed at 460 and 530 nm, respectively. Circular particles with a size of 2–7 nm were observed via TEM. Cadmium and sulfide elemental signals were detected using EDX. FTIR revealed the involvement of reactive moieties, such as carboxyl and aromatic functionalities, capping the CdS QD surface. The cytotoxic activity of the as-fabricated CdS QDs was evaluated on breast cancer MCF-7 and gastric cancer AGS cell lines via MTT assay. Remarkable suppressive and dose-dependent effects of the produced QDs were observed in the tested cells. CdS QDs exerted an enhanced influence of apoptosis on MCF-7 cells compared with that on the AGS cells.

The biogenic synthesis of a green nanohybrid made of SnO₂ QDs and carbon nanoflakes (SnO₂-CNF) was assessed [98]. The leaf extract of cogongrass (*Imperata cylindrica*) acted as a source of carbon for the preparation of CNFs via chemical vapor deposition. Similarly, the leaf extract of the golden trumpet (*Allamanda cathartica*) mediated the green synthesis of the SnO₂ QD particles. Nanoscale SnO₂ has drawn immense attention as an excellent photocatalyst due to its band gap tenability, biological and chemical inertness, good regeneration potential, and reduced nontoxicity [99]. *A. cathartica* leaf water extract comprises several phytochemicals, such as polyphenols, alkaloids, glycosides, and flavonoids. These phytochemicals are potent chelating agents because they contain polar functionalities, which may exert a chelation effect and facilitate the complexation of the Sn⁺⁴ ions during the synthesis reaction. Analysis by scanning electron microscope (SEM) revealed the presence of irregularly shaped carbon flakes with a size range of 37–41 nm. Spherical and quasi-spherical SnO₂ QD particles were equally distributed on the surface of CNFs, as revealed by the TEM images. The prepared nanohybrid was tested for its potential to degrade bisphenol A from a contaminated water sample (Fig. 1). The adsorption process was in accordance with the Langmuir isotherm and obeyed the kinetics of the pseudo second-order model. The adsorption potency reached 250 mg/g, which was ~5.3 and ~1.7 times greater than the sole use of SnO₂ QDs and CNFs, respectively.

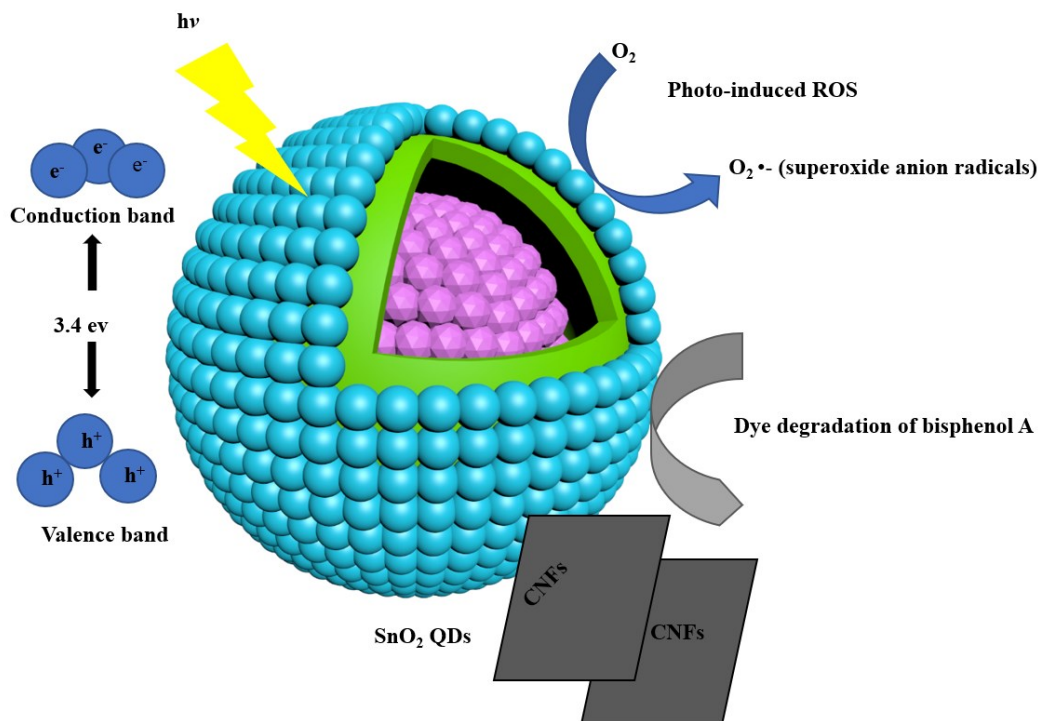


Fig. 1. Photocatalytic degradation of bisphenol A using the green synthesized SnO₂-CNFs nanohybrid.

The aqueous extract of flowers of Aparajita (*Clitoria ternatea*) was used for one-pot synthesis of SnO₂ [100]. Flavonoids and flavanols in *C. ternatea* acted as natural reductants to transform Sn²⁺ precursor ions into their nanoparticle state. Thereafter, the generated nanoparticles were oxidized, forming the SnO₂ QDs at 400°C within 2 h.

The obtained SnO₂ QDs were 7 nm in size with a spherical morphological structure and had a BEG of 3.66 eV. Upon exposure to UV irradiation, the synthesized SnO₂ QDs acted as efficient photocatalysts for the decomposition of rhodamine dye B (RhB). Based on the rate of RhB photodegradation, the SnO₂ QDs exhibited a higher photocatalytic potential than the bulk SnO₂. The RhB photodegradation rate was mainly dependent on the pH and the concentrations of H₂O₂ and SnO₂ QDs. The highest photodegradation efficacy exerted by SnO₂ QDs was achieved by using 10 mM H₂O₂ and 2 g/L SnO₂, and at pH 4.

3.2. Metal chalcogenide QDs derived from the extracts of agro-industrial wastes

CdS QDs have been synthesized using aqueous extract of the peels of papaya (*Carica papaya*) [101]. Prominent cadmium and sulfide peaks were identified via EDX. XRD analysis revealed the cubic phase of the CdS QDs. The average size of the prepared CdS QDs was in the range of 2.3–3.2 nm. Irregularly shaped particles were observed in the SEM images. Aqueous extract of the peels of pomelo (*Citrus maxima*) was tested as a green biological waste for synthesizing CdTe QDs [102]. The as-synthesized particles were highly crystalline and monodispersed with a size of 6.6 nm. Carboxyl, hydroxyl, and amino functional groups were observed in the FTIR spectrum. The phyto-fabricated CdTe QDs possessed a crystalline structure revealed via XRD. Thermogravimetric analysis (TGA) illustrated the influence of temperature on the mass of CdTe QDs. A mass change of 29.4% was observed at 300°C.

The aqueous extract of grinded watermelon (*Citrullus lanatus*) peels mediated the biological synthesis of CdS QD particles via a one-pot reaction [103]. The prepared aqueous extract was rich in carbohydrates. This was further confirmed with FTIR spectroscopy. A maximum absorption peak appeared at 484 nm with a BEG of 2.57 eV, which confirmed that the fabricated CdS particles were in the quantum confinement regime. Strong elemental signals for Cd and S with no impurities were observed using EDX. XRD patterns illustrated the hexagonal phase of the CdS QDs. The fruit sap of *Opuntia ficus-indica* acted as a green platform for the phyto-synthesis of CdS QDs [104]. FTIR revealed the presence of stretching vibrations of the C–O primary alcohol and bending vibrations of aromatic (C–H) and amino (N–H) groups. The maximum absorption peak of CdS QDs appeared at 323 nm and the BEG was 3.8 eV. The synthesized particles were cubic and crystalline in structure with no impurities. X-ray fluorescence revealed the presence of Cd (80.12%) and S (18.8%). The average particle size was estimated to be 9.56 nm.

4. Green synthesis, structural and optical properties, and versatile applications of phyto-synthesized carbon dots

Carbon dots (CDs) or carbon quantum dots (CQDs) are a class of carbonaceous nanoparticles with a size of 10 nm [105, 106]. In 2004, Xu et al. [107] discovered CDs while purifying single-walled carbon nanotubes generated via the arc-discharge technique using gel electrophoresis [108]. CDs represent the most recent addition to the carbon family. The research work of Sun et al. [109] highlighted the potential production of carbon NPs with luminescent properties. They fabricated carbon NPs and passivated them using diamine-terminated oligomeric poly (ethylene glycol). Because of the brilliant preparation, the term “carbon dots” was coined and was further used to recognize fluorescent carbon NPs [109]. CDs have gained immense interest as NPs due to their unique optical features, low toxicity, biocompatibility, ease of synthesis, and due to the availability of numerous carbon precursor sources [110, 111]. They are characterized by their superior quantum confinement regime and high solubility. Their

photoluminescent and fluorescent properties make them promising nanomaterials for application in chemical sensing, biomedicine, electro- and photocatalysis, and optoelectronic fields [112].

During the past few years, different chemical precursors such as ammonium citrate, citric acid, benzene, poly-(ethyleneimine), thiourea, and ethylene glycol were used as the common precursor materials for CD synthesis [113]; however, due to the presence of hazardous chemical solvents, exorbitant costs, and long-time reactions, their use has become restricted. Owing to these limitations, the most recent and innovative approach is to use green precursors to mediate the biological and renewable synthesis of CDs. Moreover, green sources contain significant bioactive compounds that can be carbonized to shape CDs [108]. Bioactive molecules usually exhibit various phases for CD synthesis, such as condensation, followed by polymerization, carbonization, and passivation [114]. Generation of CDs usually occurs via four main steps: (i) small sized molecules are condensed to produce intermediate chain compounds, (ii) the transitionally generated polymers become aggregated via covalent and noncovalent bonds, (iii) they are either aromatized or carbonized at elevated temperatures, and (iv) eventually the surface of the synthesized CDs is modified by several passivating and capping agents to upgrade their properties. Table 2 summarizes a list of some green-synthesized CDs using extracts of plant leaves, fruit and vegetables waste peels, synthesis techniques, reaction conditions, properties, and applications.

Table 2

Biogenic fabrication of CDs, techniques, reaction conditions, properties, and applications.

Green sources	Reaction conditions	Fluorescence color, QY (%), shape, size (nm)	Applications	References
Plant leaves				
Bamboo	Hydrothermal, 200°C, 6 h	Blue, 7.1, spherical, 2–6	Copper (II) ion detection	[115]
Willow	Hydrothermal, 180°C, 24 h	Blue, -, irregular, 2–4	Fluorescent ink, electrocatalytic application	[116]
Coriander	Hydrothermal, 240°C, 4 h	Blue, 6.48, irregular, 4.15	Antioxidants, bioimaging agent, sensor	[117]
<i>Aloe vera</i>	Carbonization, 250°C, 2 h	Blue, 16.4, spherical, 1.5–3.7	Drug delivery vehicle	[118]
Date palm	Carbonization, 300°C, 2 h	Green, 33.7, spherical, 35	Photocatalyst, antibacterial agent	[119]
<i>Ginkgo biloba</i>	Hydrothermal, 200°C, 10 h	Bright blue, 22.8, spherical, 3	Salazosulfapyridine detection	[120]
<i>Catharanthus roseus</i>	Hydrothermal-carbonization, 200°C, 4 h	Blue, 28.2, spherical, 5	Multi-ion detection and biological applications	[121]

<i>Tamarindus indica</i>	Hydrothermal, 210°C, 5 h	Blue, 46.6, spherical, 3.4 ± 0.5	Glutathione and mercury detection	[122]
Agricultural wastes (peels)				
Watermelon	Carbonization-simple filtration, 220°C, 2 h	Blue, 7.1, spherical, 2	Optical imaging probe	[123]
Pomelo	Hydrothermal, 200°C, 3 h	Green, 6.9, spherical, 2–4	Mercury ion detection	[124]
Orange	Hydrothermal-carbonization, 180°C, 12 h	Blue, 36, spherical, 2–7	Photocatalytic degradation	[125]
Onion	Heating, 120°C, 15 h	Blue, 28, spherical, 15	Multicolor imaging Sensor of Fe ⁺³ ion	[126]
Orange and lemon	Carbonization, 180°C, 2 h	Blue, 16.8/15.5, spherical, 6.5/4.5	Fe ³⁺ ion and tetrazine detection	[127]
Grapefruit	Hydrothermal, 190°C, 12 h	Blue, -, spherical, 4.2 ± 0.11	p53 protein detection	[128]
Pineapple	Hydrothermal, 150°C, 2 h	Blue, 0.42, spherical, 2–3	Sensor, memory element in security devices, mercury detection	[129]
Sweet lemon	Hydrothermal-carbonization, 180°C, 3 h.	Green, -, spherical, 1.5–6	Gene therapy and breast cancer detection	[130]
Mango	Carbonization-oxygenolysis, 300°C, 6 h	Blue, 8.5 ± 0.2, quasi spherical, 3	Fe ³⁺ ion detection, cellular labeling	[131]
Other agricultural wastes				
Banana pseudo-stem	Hydrothermal, 120°C, 2 h	Green, 48, spherical, 2–3	Bioimaging and Fe ⁺³ ion detection	[132]
Litchi pulp	Hydrothermal, -	Blue, -, irregular, 4.1	Aflatoxin B ₁ immunoassay	[133]

4.1. Green CDs derived from the extracts of different plant parts

The aqueous leaf extract of tulsi (*Ocimum sanctum*) successfully mediated the phyto-synthesis of fluorescent CDs for the first time via a facile and green hydrothermal approach [134]. The as-prepared CDs were highly photostable and generated a high QY of approximately 9.3%. The potency of *O. sanctum*-derived CDs to act as sensors for Pb⁺²

detection was further investigated. The prepared CDs displayed superior sensitivity and specificity toward Pb^{+2} ions in a real water sample. Likewise, in another study, the synthesis of highly fluorescent multifunctional CDs was derived from tulsi leaves via a hydrothermal approach [135]. Upon exposure to UV light, the prepared CDs exhibited blue fluorescence. TEM revealed the morphological structure of the prepared CDs as spherical particles with a diameter of 5 nm. The prominence of the carbon and oxygen elemental signals was detected by EDX. The chemical configuration was further confirmed via FTIR spectroscopy, which revealed the incidence of amino, hydroxyl, carbonyl, and carboxylic functional groups surrounding the surface of the tulsi-derived CDs. The graphite structure of the CDs was clearly detected by XRD. CDs were stable in the pH range of 3–10. Since heavy metal ions represent a major threat to humans, it is necessary to develop facile, sensitive, and precise techniques for accurate detection in food and the environment. In this context, the prepared CDs exhibited high selectivity for detecting Cr (VI) ions in an aqueous solution via the inner filter effect mechanism.

CDs were prepared using an aqueous leaf extract of pennywort (*Centella asiatica*). HRTEM images illustrated the formation of 2.18 nm sized spherical particles [136]. Dynamic light scattering (DLS) and atomic force microscopy (AFM) revealed that the prepared carbonaceous particles were in the nanoscale range. Maximum emission and excitation peaks were observed at wavelengths of 440 nm and 360 nm, respectively. The maximum measured QY reached 3.4%. The XRD diffraction peaks of the prepared CDs displayed two peaks at $2\theta = 28^\circ$ and 32° , in addition to three other diffraction peaks at $2\theta = 41^\circ$, 45° , and 66° . This specified the random preparation of the synthesized CDs. Moreover, the appearance of these peaks confirmed the dense packing of the graphitic carbon atoms with alkyl chains, which eventually indicated the poor crystallinity of the CDs derived from *C. asiatica*. This could be ascribed to the presence of several oxygen-containing functional groups surrounding the prepared CDs. EDX and X-ray photoelectron spectroscopy (XPS) demonstrated the abundance of carbon and oxygen elemental signaling. The FTIR findings revealed the synthesis of unsaturated carbon through the carbonization process and the abundance of different oxygen-containing functionalities (e.g., carbonyl, hydroxyl, and carboxyl) on the surface of the CD particles. The high negative zeta potential value indicated the coating of the prepared CDs with several negatively charged functionalities, which aided to the high water dispersibility of the prepared particles. Nuclear magnetic resonance confirmed the presence of a high percentage of aliphatic carbon and a small percentage of polyaromatic domains. Upon exposure to sunlight, the arylamine dye acted as an electron donor, and the electrons were photoexcited. CDs acted as electron acceptors and efficient carriers to transport these photoinduced electrons. Furthermore, electron-hole pairs were formed after the excitation of electrons, followed by release of hydroxyl radicals ($\text{OH}\cdot$). These radicals are essential for the decomposition of dyes into water, CO_2 , and other small hydrocarbons. The free energy negative value demonstrated the feasible electron transfer from arylamine dye to CDs and the promising application of *C. asiatica*-derived CDs as efficient photocatalysts.

CDs were prepared for the first time using the water extract of henna leaves (*Lawsonia inermis*) [137]. A green hydrothermal reaction was carried out using the henna extract as a carbon precursor for the fabrication of CDs without addition of any external chemicals. Fluorescence intensity was increased by increasing the reaction time to 12 h and the temperature to 180°C . TEM revealed the presence of 5 nm sized, well-dispersed, and quasi-spherical CDs. DLS evaluated the particle size distribution, which ranged from 3 to 7 nm, in agreement with the TEM data. AFM images

demonstrated that the synthesized CDs were 5 nm in size with no aggregation. EDX illustrated that the percentage of carbon exceeded that of oxygen, which indicated the amorphous structure of the phyto-synthesized CDs. Raman spectroscopy assessed the structural defects of the henna-derived CDs. The estimated Raman intensity ratio (I_D/I_G) was 0.74, which further confirmed the amorphous structure of the prepared CDs. Under ultraviolet irradiation, CDs expressed robust green fluorescence. A broad absorption spectrum was observed with the peaks ranging from 270 to 380 nm, which entirely differed from those of the fresh henna leaf extract. The maximum emission intensity was observed at 360 nm. Interestingly, no change was observed in the photostability of the henna-derived CDs for 10 months. When the antibacterial potential of the as-synthesized CDs was further evaluated against *Staphylococcus aureus* and *Escherichia coli*, the effect of CDs was higher against Gram-positive bacteria than that against Gram-negative bacteria due to the cell wall structure, which allowed less permeability of the antibacterial agent. Furthermore, henna-mediated CDs were able to detect methotrexate, which is one of the most widely used anticancer drugs in human plasma serum.

Seeds of mung bean (*Vigna radiata*) mediated the green phyto-synthesis of fluorescent CDs through a one-pot hydrothermal reaction [138]. *V. radiata* seed extract served as the sole carbon source, whereas ethylenediamine acted as a nitrogen source for doping the prepared CDs with nitrogen (N@VRCD). The prepared N@VRCD exhibited a high QY of up to 58%. Upon exposure to visible light, N@VRCD exhibited high photostability, water solubility, and a shiny multicolor fluorescence. The as-synthesized green fluorescent CDs were found to be phototoxic in the presence of sunlight due to the accumulation of ROS. They could be selected as a potent and novel chemotherapeutic agent for the treatment of tumors. Additionally, N@VRCD exhibited high detection sensitivity toward Fe^{3+} ions. Blue luminescent CDs mediated by the aqueous leaf extract of *Prosopis juliflora* acted as a dual fluorescence biosensor for the detection of mercury and chemet (i.e. anti-poisoning drug) via a facile one-pot reaction [139]. The produced QY percentages reached 5%. The mercury limit of detection under optimized conditions reached 1.26 ng mL⁻¹.

A simple, feasible, and green hydrothermal technique was applied for the synthesis of CDs using the leaf water extract of roselle (*Hibiscus sabdariffa*) [140]. The synthesized CDs were amorphous in nature with a spherical shape and a size range of 4.85–7.78 nm. UV/Vis spectrophotometer revealed an absorbance peak at 267 nm, which was ascribed to the presence of n- π^* transitional C–O bonds. The prepared CDs exhibited strong blue fluorescence upon exposure to UV light. The photoluminescence (PL) spectrum revealed a characteristic band at 429.7 nm, which was responsible for the blue fluorescence emission. *H. sabdariffa*-derived CDs acted as excellent sensors for detecting different concentrations of Cr^{6+} ions (0.01–0.05 mM).

Cannabis (*Cannabis sativa*) acetone leaf extract mediated the phyto-synthesis of CDs and Ag@CDs [141]. *C. sativa* served as the sole carbon precursor in the synthesis reaction and reduced the silver ions to Ag^0 . HRTEM images revealed that the prepared CDs were spherical in shape and 5 nm in size. An absorbance peak was identified at approximately 330 nm, which is characteristic of CDs. Another surface plasmon resonance peak appeared at 440 nm, which is characteristic of AgNPs in Ag@CDs. The antibacterial potency of the synthesized Ag@CDs was assessed against *E. coli*, *S. aureus*, and dental samples containing distinct microflora via an agar well diffusion assay and microtiter plate technique. Statistical analysis revealed that 42 mg/mL was the significant minimum inhibitory concentration (MIC) value of Ag@CDs against *S. aureus* and *E. coli* ($p < 0.0001$); however, none of the tested

concentrations of Ag@CDs (0–45 $\mu\text{g}/\text{mL}$) could be reported as MIC against the dental microflora sample. This could be ascribed to the diversity and heterogeneity of the tested culture. A schematic representation of the effect of Ag@CDs against bacterial cells is illustrated in (Fig. 2).

The antibacterial effect of CDs has gained considerable attention owing to their superior optical properties, low mammalian cell toxicity, and the potential to interact with pathogenic microorganisms. The degree of interaction between CDs and bacteria is mainly dependent on the morphology, size, and chemical surface configuration of the CDs [142]. CDs bearing a positive charge on their surface (i.e. cationic CDs) can interact via electrostatic attraction forces with the negatively charged bacterial cell membrane, which causes bacterial cell damage via cell wall deformation, protein denaturation, ROS generation, genomic DNA disruption, phospholipid release, cytoplasmic leakage, and ultimately bacterial death [143].

Hi et al. [144] reported that the morphological shape of CDs affected the antibacterial mode of action against *S. aureus* via bursting of C_{60} cage and production of C_{60} -GQDs, which displayed the nonzero Gaussian curvature. The observed antibacterial behavior was associated with GQD potential to destroy the integrity of the bacterial cell envelope. Contrary, the synthesized C_{60} -GQDs with planar geometry did not exhibit any antibacterial action against *E. coli*, *B. subtilis*, and *P. aeruginosa*. The above findings indicate that the shape of CDs could play a crucial role in determining their antimicrobial effectiveness.

Furthermore, when CDs are functionalized with noble metal nanoparticles, hybrid nanocomposites with high antimicrobial potential are produced. Travlou et al. [145] prepared nanocomposites made up of Ag-1,3,5-benzenetricarboxylic acid metal-organic frameworks (MOFs) with sulfur and nitrogen-doped CDs. The fabricated nanocomposite and hybrid materials were tested for their antibacterial activity against *B. subtilis* and *E. coli*. It was revealed that the conjugation of the composite and the hybrid materials boosted a synergistic effect which enhanced the antibacterial activity. The mechanism behind the antibacterial action was governed by the complex chemistry and unique morphology (i.e. nanorod shape). The released Ag^+ ions are known to have a high affinity towards sulfur compounds in bacterial cells. The formation of metallic Ag and AgS were suggested to be responsible for the inhibition of bacterial growth by the synthesized composite and hybrid materials.

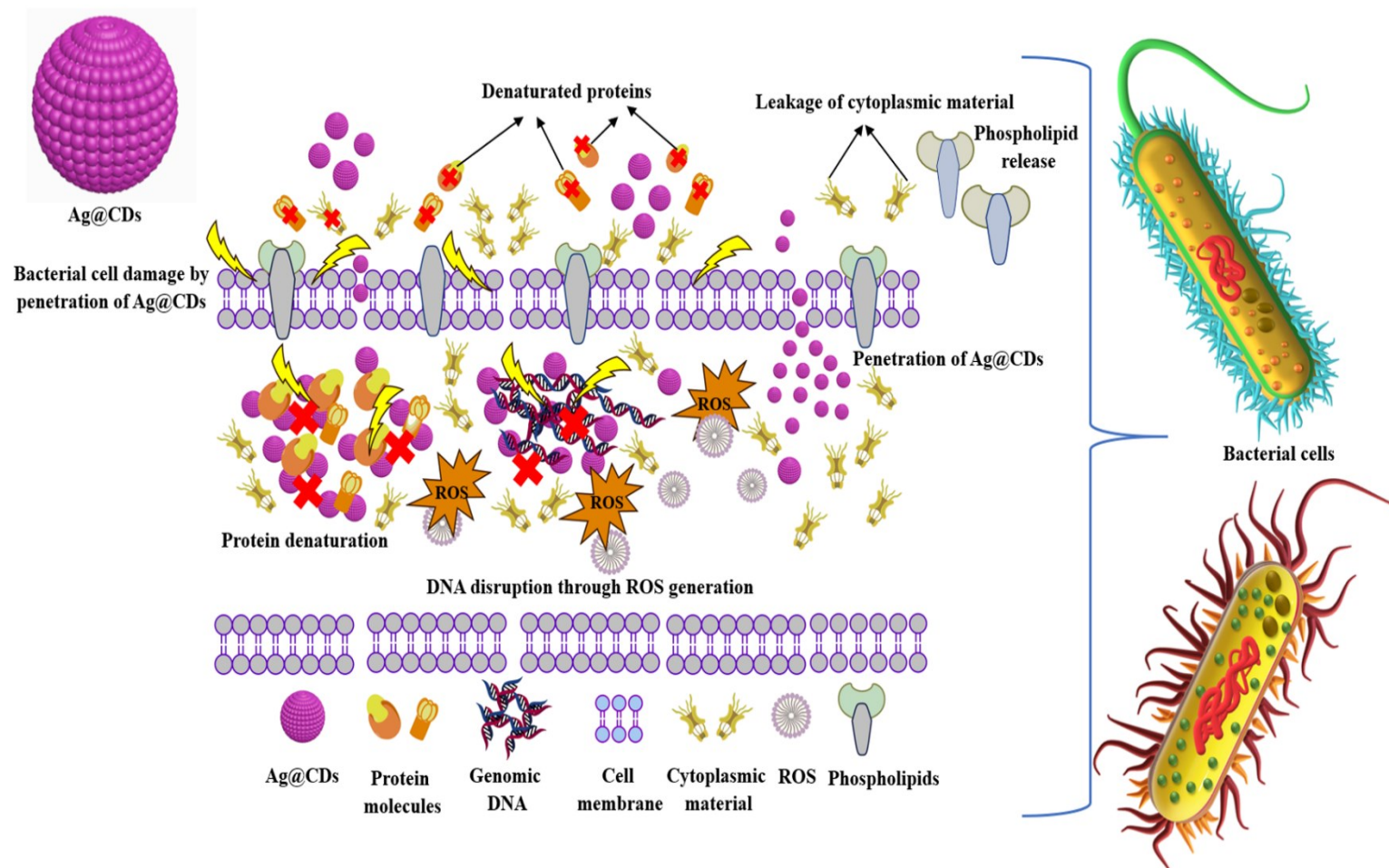


Fig. 2. Illustration of the antibacterial mechanism of action of Ag@CDs via adsorption and subsequent penetration of Ag@CDs into the bacterial cell leading to cell wall deformation, protein denaturation, ROS generation, genomic DNA disruption, phospholipids release, and cytoplasmic leakage.

Water leaf extract of mango (*Mangifera indica*) is a green and cost-effective source for the phyto-synthesis of highly fluorescent CDs via a one-pot pyrolysis reaction at 300°C for 3 h [146]. A broad absorption peak was observed at 213 nm, which presumably reflected the p-p* carbon transitions. A sharp emission peak at approximately 525 nm appeared upon excitation at 435 nm. The prepared CDs exhibited strong blue emission. Blue emission of CDs usually depends on two factors: CD internal BEG and external fluorescence. Hydrophilic (e.g., -OH and C=O) and hydrophobic (e.g., C=C and C-H) functional groups were depicted via FTIR, suggesting the amphiphilic nature of the synthesized CDs. Spherical particles with sizes of 2–10 nm were demonstrated via HRTEM. Three different peaks at 284.52, 401.7, and 532.26 eV were detected by XPS, corresponding to C1s, N1s, and O1s peaks, respectively. The structural composition percentage was found to be 92.54% for carbon, 4.29% for oxygen, and 3.15% for nitrogen. In general, the CD-sensing potential is usually affected by pH. The PL intensity of *M. indica*-derived CDs was weak under strong alkaline and acidic pH conditions (i.e., 1 and 11). This might be due to the availability of carboxylic acid groups surrounding the CD surface, which in turn hindered the recombination of the electron-hole pairs and eventually led to reduced fluorescence intensity. Moreover, under extreme acidic conditions, the protonated form of amino groups minimized the electron-donating efficacy. In contrast, under extreme alkaline conditions, the amine groups became dominant around the entire CD surface, offering high electron donation potential. Highest fluorescence intensity was obtained at pH 7. The synthesized CDs exhibited a remarkable sensing potential toward Fe²⁺ ions in the water sample and in the Livogen tablet as a realistic sample. The Fe²⁺ ion detection limit was 0.62 ppm. The synthesized CDs displayed substantial photostability for 3 months; therefore, this study offers an easy and quick methodology for CD-based detection of Fe²⁺ ions through a photoluminescent quenching effect as represented in Fig. 3.

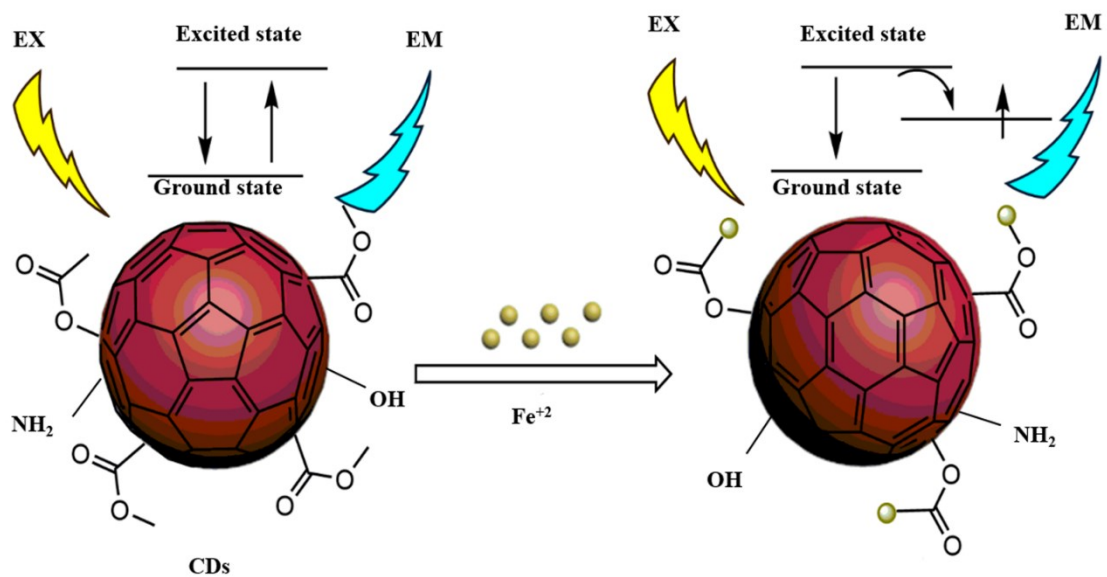


Fig. 3. Proposed quenching mechanism of the fluorescent CDs derived from *Mangifera indica* in the presence of Fe²⁺ ions.

The biological fabrication of CDs from the leaves of betel (*Piper betle*) was investigated [147]. The as-prepared CDs had the potential to detect Fe³⁺ in aqueous medium in the presence of other metal ions. In another study, grinded

grass was used to fabricate N-CDs by applying a hydrothermal reaction at 180°C for 2 h [148]. The photocatalytic potency of the N-CDs was evaluated against five dyes: acid blue, eosin y, methyl orange, acid red, methylene blue, and eriochrome black t. High photocatalytic degradation efficacy was attained under ultraviolet and visible irradiation. Furthermore, cadmium and lead ions were successfully removed in the presence of N-CDs with removal percentages of 37% and 75%, respectively.

4.2. Green CDs derived from the extracts of agro-industrial wastes

Aqueous peel extract of *Trapa bispinosa* was reported to mediate the biological synthesis of CDs [149]. After heating the *T. bispinosa* peels for 120 min at 90°C, the extract exhibited a greenish brown color due to the thermal oxidation of the existing phytochemical constituents. The synthesized CDs exhibited green luminescence under UV light. The UV/Vis spectrophotometer revealed a CD absorption peak between 400 and 600 nm. The fluorescence intensity of CDs was enhanced with an increase in wavelength excitation. The highest fluorescence intensity was recorded at 450 nm. Monodispersed and spherical CD particles were observed via HRTEM with sizes ranging from 5 to 10 nm. XRD diffraction patterns assigned the graphitic structure of the *T. bispinosa*-derived CDs. The I_D/I_G intensity ratio confirmed the purity of the as-synthesized CDs via Raman spectroscopy. FTIR illustrated the presence of –CH, –OH, and –C=C– functionalities surrounding the prepared CDs.

The generation of highly luminescent N-CDs by using the extract of unripen fruits of plum (*Prunus mume*) was investigated via a facile hydrothermal-carbonization technique [150]. When the effect of different pH (2, 3, 5, 7, and 9) was assessed on the synthesis of N-CDs, the maximum fluorescence intensity was obtained at pH 9. The average size observed by HRTEM was almost 9 nm. An inner layer space of 0.21 nm was depicted by XRD. Raman spectroscopy confirmed the graphitic structure of the prepared N-CDs. XPS and FTIR spectroscopy illustrated the nitrogen doping around the prepared CDs. The phyto-synthesized N-CDs exerted low toxic effects and were applied as staining probes for fluorescence cell imaging. In another study, the pulp of litchi (*Litchi chinensis*) was used as a source of carbon for the green synthesis of CDs via a hydrothermal approach [133]. The prepared CDs were functionalized with MnO₂ nanosheets, and the nanohybrid obtained contributed to the efficient fluorometric recognition of aflatoxin B1.

Fe³⁺ ions, one of the most common trace elements in living organisms, play a pivotal role in cellular metabolism, oxygen transport, and DNA synthesis in human body due to their simple redox chemistry and high affinity toward oxygen [151]. Abnormal levels of Fe³⁺, however, cause damage to normal physiological functions, which may lead to certain illnesses such as hemochromatosis, anemia, heart failure, hepatitis, diabetes, cancer, and arthritis [152]. Recently, QDs have been introduced as excellent fluorescent probes that can be used for accurate sensing of Fe³⁺ ions. Four types of blue fluorescent CDs, OP-CDs, B-CDs, PL-CDs, and MF-CDs were synthesized from orange peels, leaves of *Ginkgo biloba* and *Paulownia* sp., and flowers of *Magnolia virginiana*, respectively. The obtained CDs acted as efficient detectors of Fe³⁺ ions in lakes [153].

A facile hydrothermal synthesis route was applied for the green synthesis of CDs and AgNPs from the extract of unripen *Prunus mume* at 180°C for 5 h [154]. Interestingly, *P. mume* mediated the bioreduction of silver ions to AgNPs and acted as a carbon precursor for CD synthesis. The prepared AgNPs were supported on the surface of the N-CDs. The resultant nanohybrid acted as an efficient catalyst for degrading the methyl orange and methylene blue dyes. The

ability of aqueous peel extract of pomegranate (*Punica granatum*) and watermelon to mediate the phyto-synthesis of CDs was further evaluated [155]. Pomegranate extract-derived CDs (P-CDs) exhibited higher therapeutic effect than the watermelon-derived CDs (W-CDs). The antimicrobial potential of the synthesized P-CDs and W-CDs was tested against certain pathogenic strains such as *Bacillus subtilis*, *S. aureus*, *Psuedomonas aeruginosa*, *E. coli*, and *Fusarium oxysporum*. Both exhibited good antimicrobial activity against the tested pathogens.

5. Phytochemical constituents involved in QD green synthesis

Plant species with a high potential for hyperaccumulation and detoxification of heavy metal ions are the most suitable plant extracts to have the highest reduction potential and to serve as promising bio-nano-factories for the synthesis of nanoscale sized-particles [156]. Metal ion tolerance in plants can be described as the ability to thrive in soils that are phytotoxic to other plants and to manifest an association between the genotype and the surrounding environment [157]. Some plants that grow on metallurgical soils have evolved the capacity to accumulate large quantities of metals inside their tissues without showing any signs of toxicity [158]. Approximately 450 plant species have been reported as hyperaccumulators of numerous heavy metal ions and to have the capacity to reduce metal ions on their surface and even in tissues that are far from the penetration site, for instance, *Brassica juncea* (mustard greens) and *Medicago sativa* (alfalfa) [159]. Hyperaccumulators describe plants with enhanced tolerance to contaminants, allelochemicals, draught, and high resistance toward pests and pathogens [160]. Plant hyperaccumulators are capable of storing metal ions beyond their metabolic demands with concentrations of up to thousands of ppm [161]. They have a great tendency for heavy metal extraction from soil; a quick productive translocation of metals from roots to aerial parts; and a tremendous potential for detoxification and sequestration of heavy metals. Toxicity is minimized by retaining the metal ions inside vacuoles, which are characterized by low metabolic activities, thus significant metabolic activities are not impeded [162]. Plants protect themselves from metal toxicity by establishing mechanisms through which metal ions have access to cell cytosol and then the metal ions become automatically complexed in other forms or inactivated to prevent metal ions from affecting the normal functions of plant cells. Besides, plants follow homeostasis to enhance tolerance towards metal ions. Hyperaccumulator plants were reported to exhibit high expression levels of transporter genes in contrast to non-accumulator plants [163].

Terpenoids (e.g. eugenol), flavonoids (e.g. luteolin and quercetin), and amino acids (e.g. tyrosine and tryptophan) are the pivotal plant metabolites responsible for the bioreduction of metal ions [156]. Plant terpenoids are derivatives of essential oils and they are composed of volatile organic constituents. They represent the oxygenated variants of terpenes and the isoprenoid unit is the building block of terpenoids [164]. Phenolic compounds can easily bind to metal ions via carboxyl and hydroxyl moieties [165]. Flavonoids are a broad group of polyphenolic compounds comprising many classes: anthocyanins, chalcones, isoflavonoids, flavonols, flavanones, and flavones, which can effectively chelate and reduce metal ions to their nanoscale size. The diverse functions and structures of amino acids have provoked their affinity to reduce metal ions based on the suitability of their side chains [166]. Certain data have shown the role of sugars (e.g. monosaccharides, disaccharides, and polysaccharides) in reducing metal ions [167]. The aldehyde group in glucose acts as a reducing agent, while fructose contains keto-group which transforms from ketone to aldehyde form. However, the bioreduction power of disaccharides and polysaccharides depends primarily on the monosaccharide components to form an open-chain to provide an aldehyde moiety. It is extrapolated that the

functional groups of plant biomolecules are the essential agents during the formation of nanoscale-sized particles [164].

Various phytochemical compounds are found in *Lawsonia inermis* leaf water extract, including fatty acids, phenolic compounds, coumarins, naphthalene, flavonoids, gallic acid, steroids, aliphatic hydrocarbons, and quinines (Fig. 4a) [137]. These compounds contain hydroxyl, amino, carbonyl, and carboxyl functional moieties and have the potential to dehydrate under appropriate hydrothermal conditions to mediate the synthesis of CD particles. In another study, several bioactive molecules in *Malus floribunda* extract such as flavonoids, phenols, anthocyanins, and tannins were involved in the synthesis of N-CDs [9]. It was depicted that these phytochemicals might have undergone dehydration, polymerization, and carbonization throughout the hydrothermal procedure to produce N-CDs.

The extract of ripen berries of *Lantana camara* are rich in glycosides, carbohydrates, and flavonoids [168]. Once treated with alkali, glycosides form sugars. Accordingly, the hydrothermal processing of *L. camara* with ethylene diamine results in the hydrolysis, decomposition, and dehydration of glycosides and carbohydrates, followed by polymerization, aromatization, and carbonization to generate the N-CDs. The green synthesis of CDs was carried out using 6 g/75 mL of *Echinops persicus* extract at a temperature of 200°C [169]. The phytochemical constituents were thoroughly investigated. The highest phenolic (90 mg/g) and flavonoid (893 mg/g) contents were found in the acetone root and ethanolic flower extracts of *E. persicus*. Moreover, high carotenoid (3.9 µg/g) and saponin (0.7. 20 g/g) contents were found in plant leaves and roots, respectively. Furthermore, tannins, alkaloids, and anthocyanins were found to be abundant in the extracts of different parts of the whole plant.

The leaf extract of *Centella asiatica* was used to mediate the synthesis of CDs, which were further used for photocatalytic water treatment [170]. Asiaticoside, asiatic acid, phenylpropanoids, polyacetylenes, and amino acids were the main phytochemicals present in *C. asiatica* leaf extract [170]. The involvement of flavonoids, fatty acids, triterpenes, volatile oils, and phenolic compounds was demonstrated in the phytofabrication of 2.8 nm CDs using *Perilla frutescens* (L.) Britt [171]. The N-CDs derived from *P. frutescens* were successfully used for detecting silver ions. Starch, cellulose, and crude protein within the leaf extract of *Eichhornia crassipes* were involved in the green synthesis of CDs [172]. The as-synthesized CDs were used in the sensitized solar cells. The phenolic and alkaloid derivatives mediated the phytofabrication of 5–7 nm CDs using the leaf extract of *P. juliflora* [173].

The presence of oleanolic acid, ursolic acid, and carvacrol in the leaves of *Ocimum tenuiflorum* mediated the synthesis of 5–7 nm CDs, which exhibited antimicrobial potential [174] (Fig. 4b). CDs were synthesized using the leaf extract of *Psidium guajava* with the help of flavonoids, ascorbic acid, protocatechuic acid, gallic acid, and caffeic acids (Fig. 4c). [175]. The as-prepared 5–10 nm-sized CDs were used for the photocatalytic degradation of methylene blue. Polyphenolic compounds acted as the key constituents for fabricating copper QDs using the leaf extract of *M. indica*. Wasted tea leaves (*Camellia sinensis*) are rich sources of polyphenols, sugars, vitamins, caffeine, and minerals. The involvement of different phytoconstituents was reported during the fabrication of CdS QDs using the extract of wasted tea leaves [176].

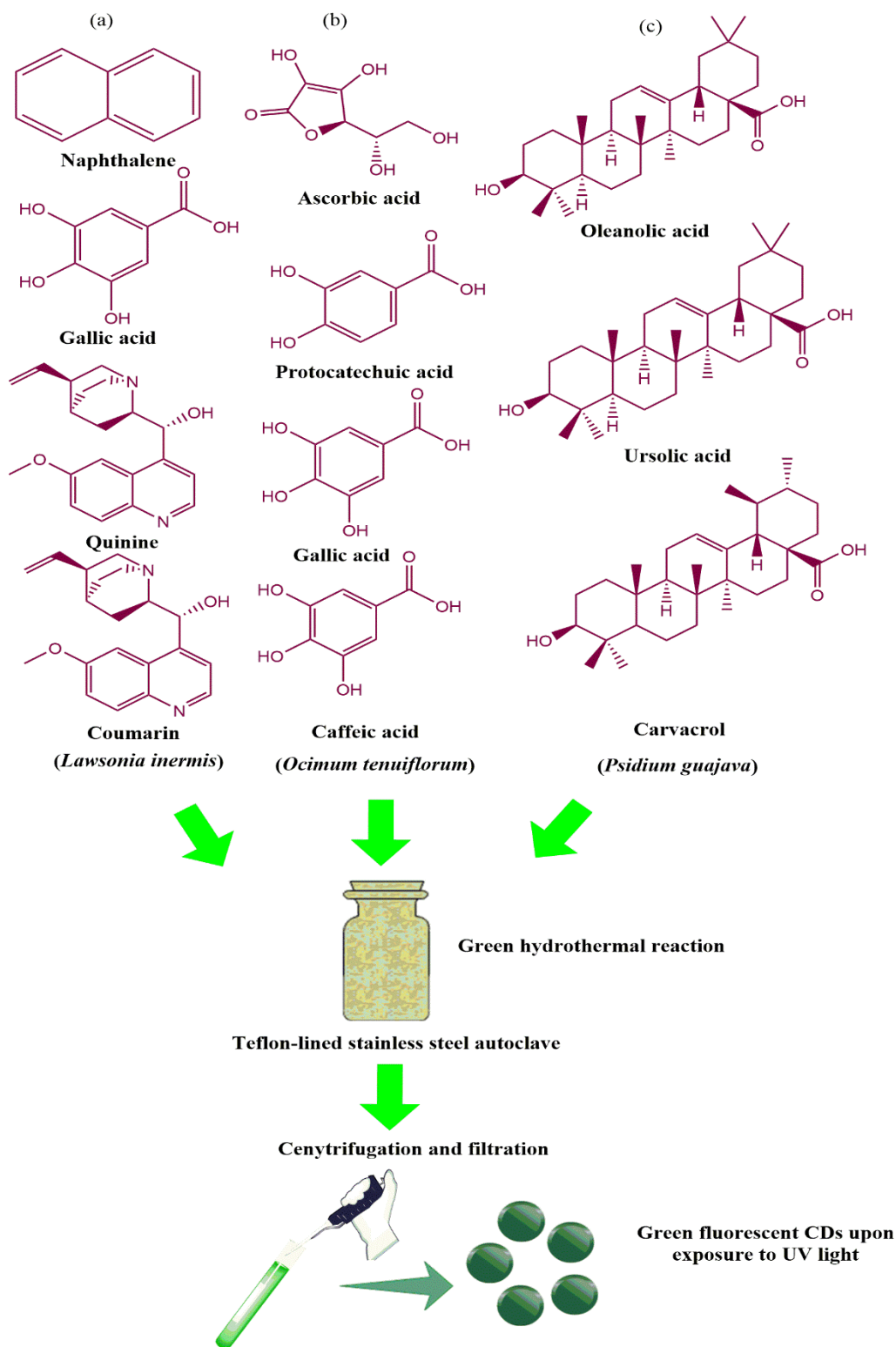


Fig. 4. Representative phytochemicals mediating one-step synthesis of green fluorescent CDs using the leaf water extracts of *Lawsonia inermis* (a), *Ocimum tenuiflorum* (b) and *Psidium guajava* (c) as raw materials via hydrothermal synthesis technique.

6. Biodistribution, biosafety, and cytotoxicity of QDs

Recently, fabrication of QDs has witnessed significant progress due to their high chemical stability, resistance to photobleaching, tunable and superior optical and electrical properties [3]. The key downside of QDs is their potential toxicity which complicates their application. Discussion of QD toxicity can be somehow confusing due to the variety of QDs being synthesized. Each category of QDs has its own distinctive physicochemical properties, which would in turn define its potential toxicity or lack thereof. QDs differ in their core and shell structure, shape, size, and surface chemistry. QD toxicity can be rationalized based on their physicochemical properties such as surface charge, ligand nature, the extent of cellular uptake, and interaction with other existing molecules in biological media [177].

Non-toxic and biocompatible QDs involve heavy metal-free QDs, carbon-, silicon-, and biomolecule-based QDs [178]. Heavy metal-free QDs have gained significant attention as alternatives for group II and IV nanocrystals because of their adverse toxic effects. Heavy metal-free ternary nanocrystals involve elements of group I (e.g., Cu, Ag), group III (e.g., Al, Ga, In, Tl), and group VI (e.g., S, Se, Te) [178] such as silver indium sulfide (AgInS_2), copper indium sulfide (CuInS_2), and zinc sulfide–silver indium sulfide (ZnS–AgInS_2). Histological, biochemical, and hematological *in vivo* toxicity tests illustrated the cytocompatibility of water-soluble indium-based QDs for biological applications following intravenous tail vein injection in rats [179]. After administration, QDs were primarily accumulated in the spleen and liver and eventually expelled from the body. This was detected over the ninety days test period using elemental analysis and complemented by photoluminescent imaging in the liver, which suggested that QD degradation took place in the liver. In another study, a comparison was conducted between the inflammatory response of two regional lymph nodes by applying different doses of $\text{CuInS}_2/\text{ZnS}$ and $\text{CdTeSe}/\text{CdZnS}$ QDs [180]. A significant difference in localized acute toxicity was observed and inflammation occurred only at a 10-fold more concentrated dose in the case of $\text{CuInS}_2/\text{ZnS}$ QDs than for their Cd-containing counterparts.

The carbon cores of CDs are non-toxic, however, their cytotoxicity depends primarily on the type and charge of functional moieties [181]. Neutral functional moieties such as polyethylene glycol have shown the least toxicity. Negatively charged functionalities (e.g., pristine) were documented to trigger cell cycle arrest, promote proliferation, and induce apoptosis. On the other hand, positively charged functionalities such as polyethyleneimine were reported to induce cell cycle arrest at G0 phase [182]. Nonetheless, these toxic effects of CDs were only observed at high concentrations ($\geq 50 \mu\text{g/ml}$) and cellular toxicity was not observed at low concentrations ($\leq 25 \mu\text{g/ml}$) [183].

In vivo studies showed that non-toxic silicic acid was generated following the biodegradation of silicon-based QDs, which can be readily excreted through urine [184]. Biomolecule-based QDs are referred to as biodots [185]. Different biomolecules can attach to QD surface via covalent linkages such as proteins, lipids, peptides, and polymer coatings. Amino acid biodots were synthesized via a green hydrothermal technique and they were found to be biocompatible. They expressed excellent intracellular absorption, which is particularly attractive for biomedical applications [186]. Phytotoxicity assessment of water-soluble methionine-functionalized CdS/ZnS QDs in *Vigna radiata* as a model plant proved its high biocompatibility [187]. Additionally, nucleotide-based biodots synthesized via one-pot hydrothermal reaction revealed long-term chemical- and photo-stability with apparent biocompatibility for therapeutic applications [188].

Core-shell functionalization is an attractive option to develop the desired QD bioactivity in biological applications [189]. Several studies have reported the toxicity of Cd-based QDs following intravenous injection in the kidney, lung, and liver [190-192]. For instance, CdTe and CdS based QDs can be potentially used for biological imaging and multifunctional drug delivery but they are known for their inherent toxicity because of the cadmium content. To reduce or eliminate their toxicity, maltodextrin and gelatin are used as proper coatings for synthesizing CdS and CdTe based nanocomposites, respectively [193]. Selenium-based QDs are usually made up of a core of CdSe, which was found to be cytotoxic mainly due to the leaching of the toxic heavy metal ion i.e. Cd (II) beside the minor concerns of Se. To overcome the toxicity of CdSe QDs, a protective coating shell of ZnS is usually employed [194]. Additionally, the cytotoxicity of QDs containing CdSe in their cores can be reduced by introducing inert coatings such as poly- (ethylene glycol) that boosts hydrophilicity and core longevity [189].

Pace et al. [195] evaluated the acute toxicity of CdSe/ZnS QDs capped with polyethylene oxide (PEO) and 11-mercaptoundecanoic acid (MUA) towards *Daphnia magna* for 48h. During the 48h observation period, PEO-coated QDs were stable and no major dissolution or aggregation occurred. Whereas, leaching of dissolved metals was noticed in the case of MUA-coated QDs. QD dose is the most important factor to determine their toxicity. In 2002, dose-dependent toxicity was first assessed by Dubertret et al. [196] via the injection of *Xenopus* frog embryos with CdSe QDs capped with ZnS and encapsulated within phospholipid micelles. No phenotypic modifications were observed at a concentration of 2×10^9 QD/cell; though, abnormalities were detected at a concentration of $>5 \times 10^9$ QD/cell.

Low clearance of QDs poses a long-term toxicity issue, specifically if repeat dosing is needed [197]. There are two primary routes for clearance of metal-containing particles, either through kidneys into urine or through the liver biliary system into feces. Fischer et al. [198] collected feces and urine samples from Sprague Dawley rats injected with 25 and 80 nm protein-coated ZnS-capped CdSe QDs. Inductively coupled plasma atomic emission spectrophotometer revealed the absence of QDs in either the two excretion routes for up to 10 days post-injection. The propensity towards QD accumulation rather than clearance tends to be true at the cellular level.

To precisely evaluate the toxicity of QDs, it is essential to classify the toxicity-correlated variants [199]. These include intrinsic factors, such as size, morphology, shape, surface features (e.g., porosity, charge, surface area, adsorbability, and roughness), agglomeration, colloidal stability, hydrophobicity/hydrophilicity, chemical structure, self-assembling, quantum regimes, crystalline nature, and contaminants. While, extrinsic parameters include dose concentration, cell/organ responsiveness, exposure paths (e.g., pulmonary, oral gavage, dermal, intravenous, subcutaneous, intramuscular, intraperitoneal, and intradermal administration), and type of animal models (e.g., mice, rats, and zebrafish) [200].

QDs affect cellular viability and differentiation, which might not occur at small doses but at high concentrations or after prolonged exposure [201]. The detrimental effects of QDs arise when the concentration and exposure time exceed the threshold levels; however, the exact threshold cannot be confirmed because it is difficult to guarantee the uniformity of different QDs from various preparation methods. Moreover, it is sometimes difficult to ascertain the disturbance threshold level of the organelles. The extent of cell injury depends on the stress intensity. Low oxidative stress usually disrupts the cellular redox homeostasis and causes inflammation in the intermediate oxidative milieu. Large oxidative bursts lead to cytotoxicity and even cell death [202]. The cytotoxicity, which may be caused by QDs,

714 is schematically represented in (Fig. 5). It is speculated that most QDs exhibit cytotoxic effects both *in vivo* and *in*
715 *vitro* only after the degradation of the surrounding surface coating. The biodegradation of the QD surface coating is
716 time-dependent and a relatively slow process [203].

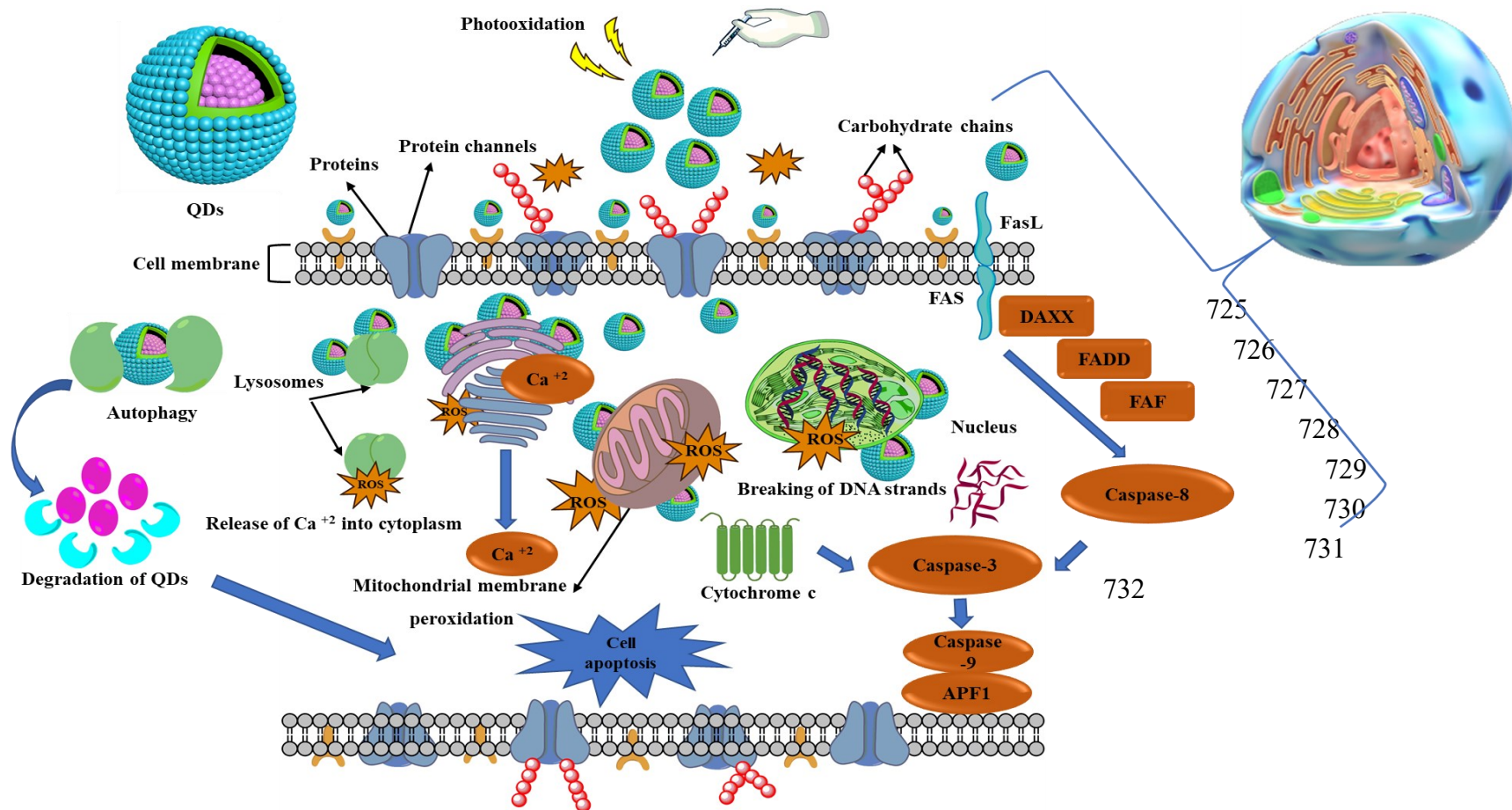


Fig. 5. Schematic representation of cytotoxicity caused by metal chalcogenide QDs on cancer cell lines. Occurrence of morphological alterations inside the cell including: excessive generation of ROS, elevation of intracellular levels of Ca^{+2} , DNA damage, mitochondrial dysfunction, auto-phagocytosis, stress on endoplasmic reticulum, disruption of inside organelles, and cell apoptosis. (Abbreviations: ROS: Reactive Oxygen Species, DAXX: Death Associated Protein 6, FADD: Fas-associated Protein with Death Domain, FAF: Fas-associated Factor 1, APF1: ATP-dependent Proteolysis Factor 1, Caspases: Group of Protease Enzymes having a Crucial Role in Cell Apoptosis or Autophagy).

The cellular interaction and uptake of CdTe QDs capped with gelatinized and nongelatinized thioglycolic acid were assessed [204]. The assessment was performed on PC12 cells using confocal laser microscopy. The QD-cell interaction was recognized by varying QD concentrations with different incubation periods up to 72 h. Moreover, DNA quantitative measurements and cell differentiation experiments were performed to compare the factors that might lead to cell stress and, eventually, cell death. When stabilized CdTe QDs were co-incubated with PC12 cells, particles acted as excellent fluorophores, with the capability to illuminate the cell cytoplasm with no lethal effects at concentrations of approximately 10^{-9} M. Three different assays were performed to track the cellular functions, including cell viability, DNA quantification, and DNA proliferation. The cell response was not only concentration-dependent but also regulated by the surrounding capping surface of the prepared QDs. Gelatin capping acted as a barrier against the leakage of toxic atoms; thus, minimizing the negative impact of the tested QDs. The cytotoxicity of *O. sanctum*-derived CDs was evaluated in MDA-MB 468 cells via MTT assay [134]. The CDs were distributed completely and homogeneously across the cell membrane, cytoplasm, and cell nucleus; therefore, they can serve as potential candidates for imaging MDA-MB 468 cells. The cytotoxic effects of some metal chalcogenide QDs on different cell lines are summarized in Table 3.

Table 3

Types, size, and exposed concentration of various metal chalcogenide QDs on different cell lines.

Type of metal chalcogenide QDs	Size (nm)	Cell lines	Exposed concentrations	References
CdSe	4	Hepa1-6	5, 10, and 20 nM	[205]
CdTe	5	HeLa	5 mg/mL	[206]
	2.2	AML12	0–40 μ g/mL	[207]
	5.06 \pm 0.98	HepG2	0–400 μ g/mL	[208]
	5	HepG2	0–100 μ g/mL	[209]
CdS	2–5	A549	10–50 μ g/mL	[210]
	1.4–1.6	HEK293	1 mg/L	[211]
ZnS:O	2–5	Hela	0–200 mg/mL	[212]
MoS ₂	2.2 \pm 0.6	NRK	0.25–1 mg/mL	[213]

CDs derived from the extract of *Trapa bispinosa* exhibited excellent biocompatibility toward Madin–Darby canine kidney (MDCK) cells [149]. They did not exert any lethal effect on the tested MDCK cell line at the concentration range of 1–3 μ g/mL. At 3 μ g/mL, approximately 80.32% of the cells remained viable. In another study, N-CDs derived from *Hylocereus undatus* were evaluated for their cytotoxic potential and biocompatibility on both MCF-7 and L-929 cell lines. At high concentration of N-CDs (i.e., 50 μ L/mL), the cell viability was 81% and 90% for MCF-7 and L-929 cell lines, respectively [214]. The prepared N-CDs exhibited passive diffusion and endocytosis mechanisms toward MCF-7 and L-929 cells [215]. When the cytotoxic potential of *L. camara* CDs was investigated in HEK-293 and MCF-7 cells, exceptional high biocompatibility was observed [168]. Consequently, these CDs can

hold strong potential to act as biological imaging agents due to their high excitation and fluorescence tunable emissions.

The cytotoxicity of CdS QDs derived from the aqueous extract of waste tea leaves (*Camellia sinensis*) was evaluated against MCF-7 cells [176]. The polyphenolic coating surrounding the CdS particles collaborated with the prepared QDs to generate ROS. ROS generation induced apoptosis of the MCF-7 cell line. Flow cytometry and fluorescence staining analysis were employed to further understand the cytotoxic activity of the as-synthesized CdS QDs. The flow cytometry data illustrated the induction of MCF-7 cells by the CdS QDs through cell cycle arrest at two phases, S and G2/M. Modulation of apoptotic and anti-apoptotic proteins aided in the interpretation of the possible apoptosis mechanism by using Western blot analysis. The apoptotic and anti-apoptotic proteins were Bax, p53, caspase-3, and Bcl-2. Bax, p53, and caspase-3 were perfectly regulated, whereas the Bcl-2 protein was inappropriately regulated. The Bcl-2 improper regulation revealed the poor cytoprotection of MCF-7 cells. Moreover, the apoptotic upregulation of Bax exerted multiple changes in the cytoplasmic matrix and the mitochondrial outer membrane. The as-synthesized CdS QDs can be exploited as dual-functional therapy and delivery carrier for the treatment of tumors.

The cytotoxic activity of CDs derived from the peel extract of pomegranate (P) and watermelon (W) was evaluated via the MTT assay against HepG2 and MCF-7 cancer cells [155]. Two reference drugs were used: oxaliplatin and camptothecin for MCF-7 and HepG2 cells, respectively. The IC₅₀ value was recorded as 50 µg/mL for both CDs on HepG2 and MCF-7 cells. The viability of cells decreased as the concentration of CDs increased. P-CDs exhibited a greater viability on MCF-7 cells than on Hep-G2 cells. In contrast, in the case of W-CDs, cell viability almost decreased in the same range for both cell line types. Thus, they could be used as potential anticancer agents. Both CD types were biocompatible, as they achieved a 50% decrease in tested cancerous cells at a very reduced dose of 50 µg/mL. This was attributed to the separation of CDs into cations and anions, while both HepG2 and MCF-7 cell lines held negative charges. In general, cancerous cell metabolism is usually nine times higher than the normal cell metabolism. Thus, these cells strive for several constituents from the surrounding medium, which explains the adhesion of the as-synthesized CDs to both cell line types.

CDs penetrate cancer cells via endocytosis and pass through the cell membrane without modifying the cell integrity. CDs might produce ROS in abundance, which may lead to intracellular protein denaturation, lipid peroxidation, mitochondrial dysfunction, and cell apoptosis or necrosis. Another possible mechanism behind the apoptosis of the cancer cell lines was that the membrane potential was more negatively charged than that of the normal cells. Consequently, cancer cells exhibit high uptake of CDs due to the strong electrostatic forces between cancer cell mitochondria and CDs, causing mitochondrial impairment and subsequent cell death.

The cytotoxic effects of *H. sabdariffa*-derived CDs on the breast tumor cell MDA-MB 231 indicated that the CDs were nontoxic even at high concentrations (i.e., 500 mg/mL) with an IC₅₀ value of 94 mg/mL [140]. Bioimaging of MDA-MB 231 cells confirmed that the CDs were confined only within the cellular membrane and the cytoplasmic matrix and not in the cell nucleus. Thus, the prepared CDs could be used as efficient bioimaging agents without having any adverse effects on the cell life.

The nanoconjugates made up of CdS QDs and functionalized with amino polysaccharides as shell-capping ligands had an *in vitro* cytotoxic response [216]. The cytotoxic effect was exerted in a concentration- and time-dependent

manner. Furthermore, cell viability was remarkably influenced by the cell type. Both SAOS and HEK293T cell lines had high sensitivity to the CdS-conjugates; however, non-Hodgkin's B lymphoma cells had less sensitivity toward CdS-conjugates. Unexpectedly, no toxic effects of CdS nanoconjugates were noticed by *in vivo* intravenous injection in BALB/c mouse models up to 30 d. Nevertheless, confined fluorescence was identified in *ex vivo* samples of liver tissue. Consequently, these findings proved that there is no assurance of the "risk free" *in vivo* application of Cd nanoconjugates, even if they are coated with biopolymeric ligands like chitosan, as this might cause an intolerable risk at increased concentrations and long contact period.

The biodistribution and biotoxicity of indium QDs were tested *in vivo* using rats after intravenous inoculation [179]. When the biodistribution was evaluated for 90 d, QDs were largely accumulated in both the spleen and liver. No organ dysfunction or disruption was observed in the QD-treated rats at different time points (i.e., 24 h; 1 and 4 weeks) following intravenous administration at concentrations of 12.5 or 50 mg/kg. These results suggest that indium-based QDs have lower toxicity than other metal-based QDs.

The influence of CdTe QDs on the reproductive organs of male rats was investigated at elevated (i.e., 2.0 nmol/L) and reduced (i.e., 0.2 nmol/L) concentrations per mouse [217]. Measurements of body weight presented no obvious toxic effects for the low concentrations after exposure for 90 d, but the high concentration of CdTe QDs affected the body weight after exposure for 15 d. Moreover, accumulation of CdTe QDs in the testes resulted in tissue damage at both doses on Day 90. In the meantime, either of the two treatment doses markedly affected the sperm count, but the high concentration of CdTe QDs resulted in a decrease in the sperm quality on Day 60. Nonetheless, mating the female mice with the treated male mice did not affect their pregnancy percentage, which did not differ in those mated with the untreated male mice either. These findings suggest that CdTe QDs have toxic effects on the testes depending on the applied dose. The low concentration of CdTe QDs was comparatively safe for the male mice reproductive system. The initial findings of this research allowed a deeper evaluation of the reproductive toxicity caused by Cd-containing QDs and offered a new aspect of their utilization in environmental and biological applications.

The biotoxic effects of exposing mice to CdTe QDs were investigated during pregnancy [218]. CdTe QDs were injected on Day 13 of growth. On the 20th gestational day, structural and histological characteristics of 121 fetuses were analyzed. The QD doses that affected embryonic toxicity were 5, 10, and 20 mg/kg, with fetal survival rates of 97%, 86%, and 43%, respectively. Moreover, exposure to CdTe QDs also caused a reduction in fetal length and body mass, disturbed limb ossification, and led to placental tissue impairment. QDs did not exhibit any retarding effects at the tested concentrations when analyzed using a stereomicroscope. Embryogenesis was hindered due to placental dysfunction rather than QD dispersion and accumulation in the tested fetuses. These findings suggest that mother mice were endangered by exposure to QDs during gestation.

7. Reproducibility and stability of QDs

Reproducibility is referred to as the potency of a synthesis process to generate consistent properties of a target material [10]. However, the major limitation of QD widespread use is the reproducibility of their properties during synthesis. For this reason, strict control over the synthesis parameters is needed to obtain QDs with consistent properties. By controlling different synthesis parameters such as temperature and concentration of reagents, obtaining QDs with reproducible features will be a facile process. Automation can largely help to obtain QDs with a high level

of reproducibility. Alteration of QD surface imparts reproducibility and long-term stability to QDs [219]. The stability of QDs can be boosted by appropriate engineering of shell and ligands to overcoat the QD core and to protect against air, heat, humidity, high energy, extremely acidic and basic conditions, and light [220]. QD shells play a key role in determining QD optical properties such as degree of color purity, QY, and stability [221]. Nonetheless, the overcoating should be optimized to prevent loss of QY and changes in wavelength.

QD photo- and thermal- stability can be increased by the introduction of intermediate shells, which helps to reduce any mismatching between QD core and shell [222]. Kim et al. [223] reported that the introduction of GaP intermediate shell coating to InP-derived QD particles rendered passivation and increased PL stability of InP/GaP/ ZnS QDs to 90%, whereas InP/ZnS QDs maintained only 10% of their PL intensity. Moreover, introduction of composition gradients in alloyed core@shell structures minimizes the gradual difference between the core and shell chemical structures [224]. QD stability can also be promoted by introducing inorganic or oxide over coatings; however, aggregation must be managed to prevent any decrease in QY or any redshift.

Furthermore, when shell thickness is increased, the chemical-, thermal-, and photostability are increased. For instance, the increase in shell thickness of CdSe@ZnS QDs by 1.9 nm resulted in increasing the QY from 44% to 88% [225]. Another important approach that could help to improve photo- and thermal- stability of QDs is to create strong bonds with ligands. Ligands with long chains stabilize the surface of QDs by the formation of strong bonding between the ligand anchoring functional groups and the QD particles. Manufactured films of QDs within a polymeric matrix such as polyethylene beads have shown no regression of PL strength for 7d [226]. These measures could allow the reproducibility and stability of QDs and to maintain their initial PL under harsh conditions.

8. Conclusions, challenges, and future perspectives

Phyto-synthesis of QDs is a promising and multidisciplinary domain aiming to produce QDs, using the extracts of different plant parts and agro-industrial wastes. Agricultural wastes are readily available, cost-effective, and potentially hazardous to human health and the environment. Biovalorization of agricultural waste is a promising approach for reducing excess waste and turning it into valuable materials such as QDs. This approach opens new avenues for waste management and for reducing the use of chemicals and the release of toxic byproducts.

Semiconductor QDs have been established as innovative ground-breaking platforms for several applications. Using green precursors is advantageous for the potential synthesis of highly luminescent metal chalcogenide QDs and CDs based on their respective properties and applications. Green synthesis is the need of the hour because plants and agricultural wastes contain numerous phytochemicals which can safely mediate the synthesis of QDs. Such components possess several functionalities that facilitate the reactivity, solubility, dispersibility, and stability of QDs. In this review, the phyto-synthesis of metal chalcogenide QDs and CDs using extracts of different plant parts and agricultural wastes is discussed. It also summarizes the morphological and structural properties of the phyto-synthesized metal chalcogenide QDs and CDs. Moreover, the roles of the phytochemical constituents during the synthesis process are explained. The phyto-fabricated metal chalcogenide QDs and CDs have the potential to act as sensors for heavy metal ion detection, photocatalytic degraders of dyestuffs, and antioxidant scavengers. The cyto- and biotoxicity concerns of using metal chalcogenide QDs and CDs are discussed based on their evaluation toward different cancer cell lines and animal models. There is no affirmation for the complete safety of metal cores containing

QDs, particularly for biomedical applications, due to the possible release and accumulation of metals inside the cells and organs.

Certain limitations constrain the commercial production of QDs, which involve: (i) searching for effective protocols and techniques to achieve high production rates, (ii) optimizing the synthesis parameters and monitoring the produced yield for upscale production, (iii) controlling the relative increase in the sizes of QDs after processing, (iv) monitoring the synthesis stages such as nucleation, crystallization, and growth to generate small-sized particles with high QY yield, and (v) selecting biocompatible surface functional moieties and ligands during QD synthesis.

Another important issue for CDs is that their absorption and emission wavelengths occur in the UV region; however, this issue restricts the biomedical applications of CDs, as UV light causes protein and DNA denaturation. In contrast, near-infrared light is more advantageous than UV light because it penetrates deeper in the tissues and decreases any possible fluorescence interference. Hence, synthesizing CDs compatible with the near-infrared light and satisfying the criteria required for multifunctional bioimaging applications can be a huge challenge.

Future studies should be directed toward (i) determining the effects of long-term exposure to low doses of QDs; (ii) evaluating the risk management resulting from QD preparation, handling, and storage; (iii) simplifying the synthesis protocols for fabrication of high-quality QDs; (iv) increasing the reproducibility and stability of QDs; and (v) designing microreactors, which can have better control over reaction dynamics.

Declaration of competing interest

The authors declare no conflict of interest.

Acknowledgment

This research was funded by the Ministry of Education-the Basic Science Research Program through the National Research Foundation of Korea (NRF), grant number NRF-2019R1F1A1052625.

References

- [1] J. Huang, J. Liu, J. Wang, Optical properties of biomass-derived nanomaterials for sensing, catalytic, biomedical and environmental applications, *TrAC - Trends Anal. Chem.* 124 (2020) 115800–115818. <https://doi.org/10.1016/j.trac.2019.115800>.
- [2] G.R. Bardajee, Z. Hooshyar, Probing the interaction of a new synthesized CdTe quantum dots with human serum albumin and bovine serum albumin by spectroscopic methods, *Mater. Sci. Eng. C.* 62 (2016) 806–815. <https://doi.org/10.1016/j.msec.2016.02.022>.
- [3] M. Abdel-Salam, B. Omran, K. Whitehead, K.-H. Baek, Superior properties and biomedical applications of microorganism-derived fluorescent quantum dots, *Molecules.* 25 (2020) 4486–4513. <https://doi.org/10.3390/molecules25194486>.
- [4] V.G. Reshma, P. V Mohanan, Quantum dots : Applications and safety consequences, 205 (2019) 287–298. <https://doi.org/10.1016/j.jlumin.2018.09.015>.
- [5] F. Mirnajafizadeh, D. Ramsey, S. McAlpine, F. Wang, P. Reece, J.A. Stride, Hydrothermal synthesis of highly luminescent blue-emitting ZnSe(S) quantum dots exhibiting low toxicity, *Mater. Sci. Eng. C.* 64 (2016) 167–172. <https://doi.org/10.1016/j.msec.2016.03.061>.
- [6] E. Soheyli, B. Ghaemi, R. Sahraei, Z. Sabzevari, S. Kharrazi, A. Amani, Colloidal synthesis of tunably

- luminescent AgInS-based/ZnS core/shell quantum dots as biocompatible nano-probe for high-contrast fluorescence imaging, Mater. Sci. Eng. C. 111 (2020) 110807–110818. <https://doi.org/10.1016/j.msec.2020.110807>.
- [7] M.F. Frasco, N. Chaniotakis, Bioconjugated quantum dots as fluorescent probes for bioanalytical applications, Anal. Bioanal. Chem. 396 (2010) 229–240. <https://doi.org/10.1007/s00216-009-3033-0>.
- [8] C. Zhu, Z. Chen, S. Gao, B.L. Goh, I. Bin Samsudin, K.W. Lwe, Y. Wu, C. Wu, X. Su, Recent advances in non-toxic quantum dots and their biomedical applications, Prog. Nat. Sci. Mater. Int. 29 (2019) 628–640. <https://doi.org/10.1016/j.pnsc.2019.11.007>.
- [9] R. Atchudan, T.N.J.I. Edison, S. Perumal, N. Muthuchamy, Y.R. Lee, Eco-friendly synthesis of tunable fluorescent carbon nanodots from *Malus floribunda* for sensors and multicolor bioimaging, J. Photochem. Photobiol. A Chem. 390 (2020) 112336–112346. <https://doi.org/10.1016/j.jphotochem.2019.112336>.
- [10] S. Pandey, D. Bodas, High-quality quantum dots for multiplexed bioimaging: A critical review, Adv. Colloid Interface Sci. 278 (2020) 102137–102153. <https://doi.org/10.1016/j.cis.2020.102137>.
- [11] Y. Mo, Y. Tang, F. Gao, J. Yang, Y. Zhang, Synthesis of fluorescent CdS quantum dots of tunable light emission with a new in situ produced capping agent, Ind. Eng. Chem. Res. 51 (2012) 5995–6000. <https://doi.org/10.1021/ie201826e>.
- [12] S. Mathew, Phytonanotechnology: A historical perspective, current challenges, and prospects. Phytonanotechnology: Challenges and Prospects. Elsevier Inc., United States, 2020. <https://doi.org/10.1016/B978-0-12-822348-2.00001-2>.
- [13] K.B. Narayanan, N. Sakthivel, Green synthesis of biogenic metal nanoparticles by terrestrial and aquatic phototrophic and heterotrophic eukaryotes and biocompatible agents, Adv. Colloid Interface Sci. 169 (2011) 59–79. <https://doi.org/10.1016/j.cis.2011.08.004>.
- [14] P. Dorishetty, N.K. Dutta, N.R. Choudhury, Bioprintable tough hydrogels for tissue engineering applications, Adv. Colloid Interface Sci. 281 (2020) 102163–102186. <https://doi.org/10.1016/j.cis.2020.102163>.
- [15] P. Wang, E. Lombi, F.J. Zhao, P.M. Kopittke, Nanotechnology: A new opportunity in plant sciences, Trends Plant Sci. 21 (2016) 699–712. <https://doi.org/10.1016/j.tplants.2016.04.005>.
- [16] G.E.J. Poinern, D. Fawcett, Food Waste Valorization: New Manufacturing Processes for Long-Term Sustainability, Elsevier, 2018. <https://doi.org/10.1016/B978-0-12-812687-5.22274-0>.
- [17] B.A. Omran, Biosynthesized Nanomaterials via Processing of Different Plant Parts (Phytonanotechnology) and Biovalorization of Agro-Industrial Wastes to Nano-Sized Valuable Products, in: Nanobiotechnology A Multidisciplinary Field of Science, Springer, 2020: pp. 145–184.
- [18] Z. Duan, C. Scheutz, P. Kjeldsen, Trace gas emissions from municipal solid waste landfills: A review, Waste Manag. 119 (2021) 39–62. <https://doi.org/10.1016/j.wasman.2020.09.015>.
- [19] M. Shah, D. Fawcett, S. Sharma, S. Tripathy, G. Poinern, Green synthesis of metallic nanoparticles via biological entities, Materials (Basel) 8 (2015) 7278–7308. <https://doi.org/10.3390/ma8115377>.
- [20] B.A. Omran, H.N. Nassar, N.A. Fatthallah, A. Hamdy, E.H. El-Shatoury, N.S. El-Gendy, Waste upcycling of *Citrus sinensis* peels as a green route for the synthesis of silver nanoparticles, Energy Sources, Part A Recover.

Util. Environ. Eff. 2017;40:227–236. <https://doi.org/10.1080/15567036.2017.1410597>.

[21] U.A. Rani, L.Y. Ng, C.Y. Ng, E. Mahmoudi, A review of carbon quantum dots and their applications in wastewater treatment, *Adv. Colloid Interface Sci.* 278 (2020) 102124–102148. <https://doi.org/10.1016/j.cis.2020.102124>.

[22] Z. Usmani, M. Sharma, Y. Karpichev, A. Pandey, R. Chandra Kuhad, R. Bhat, R. Punia, M. Aghbashlo, M. Tabatabaei, V.K. Gupta, Advancement in valorization technologies to improve utilization of bio-based waste in bioeconomy context, *Renew. Sustain. Energy Rev.* 131 (2020) 109965–109981. <https://doi.org/10.1016/j.rser.2020.109965>.

[23] M. Tobiszewski, J. Namieśnik, A. Mechlińska, Green analytical chemistry — theory and practice, *Chem Soc Rev* 39 (2010) 2869–2878. <https://doi.org/10.1039/B926439F>.

[24] B.A. de Marco, B.S. Rechelo, E.G. Tótolí, A.C. Kogawa, H.R.N. Salgado, Evolution of green chemistry and its multidimensional impacts: A review, *Saudi Pharm. J.* 27 (2019) 1–8. <https://doi.org/10.1016/j.jsps.2018.07.011>.

[25] R.H. Lutts, Chemical fallout: Rachel Carson’s Silent Spring, radioactive fallout, and the environmental movement, *Environ. Rev. ER.* 9 (1985) 211–225. <https://doi.org/10.2307/3984231>.

[26] P.T. Anastas, Green chemistry and the role of analytical methodology development, *Crit. Rev. Anal. Chem.* 29 (1999) 167–175. <https://doi.org/10.1080/10408349891199356>.

[27] N.J. O’Neil, S. Scott, R. Relph, E. Ponnusamy, Approaches to incorporating green chemistry and safety into laboratory culture, *J. Chem. Educ.* (2020), <https://doi.org/10.1021/acs.jchemed.0c00134>.

[28] Z. Zhao, Y. Li, Developing fluorescent copper nanoclusters: Synthesis, properties, and applications, *Colloids Surf. B Biointerfaces.* 195 (2020) 111244–111255. <https://doi.org/10.1016/j.colsurfb.2020.111244>.

[29] M. Shaker, R. Riahifar, Y. Li, A review on the superb contribution of carbon and graphene quantum dots to electrochemical capacitors’ performance: Synthesis and application, *FlatChem.* 22 (2020) 100171–100193. <https://doi.org/10.1016/j.flatc.2020.100171>.

[30] S.A.M. Zobir, S.A. Rashid, T. Tan, Recent development on the synthesis techniques and properties of graphene derivatives, Elsevier Inc., United States, 2018. <https://doi.org/10.1016/B978-0-12-815757-2.00004-8>.

[31] M. Pan, X. Xie, K. Liu, J. Yang, L. Hong, S. Wang, Fluorescent carbon quantum dots-synthesis, functionalization and sensing application in food analysis, *Nanomaterials.* 10 (2020) 930–955. <https://doi.org/10.3390/nano10050930>.

[32] P. Iqbal, J.A. Preece, P.M. Mendes, Nanotechnology: The “top-down” and “bottom-up” approaches, *Supramolecular Chemistry: From Molecules to Nanomaterials*, Wiley, New York, United States (2012). <https://doi.org/10.1002/9780470661345.smc195>.

[33] L. Liu, Z. Mi, Q. Hu, C. Li, X. Li, F. Feng, Green synthesis of fluorescent carbon dots as an effective fluorescence probe for morin detection, *Anal. Methods.* 11 (2019) 353–358. <https://doi.org/10.1039/C8AY02361A>.

[34] W. Ahmed, A. Elhissi, K. Subramani, Introduction to nanotechnology, Elsevier Inc., 2012.

https://doi.org/10.1016/B978-1-4557-3127-5.00001-5.

- [35] O.P. Bolade, A.B. Williams, N.U. Benson, Green synthesis of iron-based nanomaterials for environmental remediation: A review, *Environ. Nanotechnology, Monit. Manag.* 13 (2020) 100279–100285. <https://doi.org/10.1016/j.enmm.2019.100279>.
- [36] N. Bruna, B. Collao, A. Tello, P. Caravantes, N. Díaz-Silva, J.P. Monrás, N. Órdenes-Aenishanslins, M. Flores, R. Espinoza-Gonzalez, D. Bravo, J.M. Pérez-Donoso, Synthesis of salt-stable fluorescent nanoparticles (quantum dots) by polyextremophile halophilic bacteria, *Sci. Rep.* 9 (2019) 1–13. <https://doi.org/10.1038/s41598-018-38330-8>.
- [37] M. Ashengroph, A. Khaledi, E.M. Bolbanabad, Extracellular biosynthesis of cadmium sulphide quantum dot using cell-free extract of *Pseudomonas chlororaphis* CHR05 and its antibacterial activity, *Process Biochem.* 89 (2020) 63–70. <https://doi.org/10.1016/j.procbio.2019.10.028>.
- [38] J. Brooks, D.D. Lefebvre, Optimization of conditions for cadmium selenide quantum dot biosynthesis in *Saccharomyces cerevisiae*, *Appl. Microbiol. Biotechnol.* 101 (2017) 2735–2745. DOI 10.1007/s00253-016-8056-9.
- [39] K. Cao, M.M. Chen, F.Y. Chang, Y.Y. Cheng, L.J. Tian, F. Li, G.Z. Deng, C. Wu, The biosynthesis of cadmium selenide quantum dots by *Rhodotorula mucilaginosa* PA-1 for photocatalysis, *Biochem. Eng. J.* 156 (2020) 107497–10758. <https://doi.org/10.1016/j.bej.2020.107497>.
- [40] P. Uddandara, R. Mohan B, ZnS semiconductor quantum dots production by an endophytic fungus *Aspergillus flavus*, *Mater. Sci. Eng. B Solid-State Mater. Adv. Technol.* 207 (2016) 26–32. <https://doi.org/10.1016/j.mseb.2016.01.013>.
- [41] S. Cárdenas, D. Issell, M. Gomez-Ramirez, N.G. Rojas-Avelizapa, M.A. Vidales-Hurtado, Synthesis of cadmium sulfide nanoparticles by biomass of *Fusarium oxysporum* f. sp. *lycopersici*, *J. Nano Res.* 46 (2017) 179–191. <https://doi.org/10.4028/www.scientific.net/JNanoR.46.179>.
- [42] C. Zhang, Y. Xiao, Y. Ma, B. Li, Z. Liu, C. Lu, X. Liu, Algae biomass as a precursor for synthesis of nitrogen- and sulfur-co-doped carbon dots : A better probe in Arabidopsis guard cells and root tissues, *J. Photochem. Photobiol. B Biol.* 174 (2017) 315–322. <https://doi.org/10.1016/j.jphotobiol.2017.06.024>.
- [43] H. Elsayed, M.A. Farghali, M.A. Hassan, K. El-sayed, M. Canonico, G. Konert, K. Farroh, H.A. Elshoky, R. Ka, Ecotoxicology impact of silica-coated CdSe / ZnS quantum dots internalized in *Chlamydomonas reinhardtii* algal cells, *666* (2019) 480–489. <https://doi.org/10.1016/j.scitotenv.2019.02.274>.
- [44] A.M. Alex, M.D. Kiran, G. Hari, A. Krishnan, J.S. Jayan, A. Saritha, Carbon dots: A green synthesis from *Lawsonia inermis* leaves, *Mater. Today Proc.* 26 (2019) 716–719. <https://doi.org/10.1016/j.matpr.2019.12.409>.
- [45] Z. Gholami, M. Dadmehr, N.B. Jelodar, M. Hosseini, One-pot biosynthesis of CdS quantum dots through in vitro regeneration of hairy roots of *Rhaphanus sativus* L . and their apoptosis effect on MCF-7 and AGS cancerous human cell lines (2020) 015056–015067. <https://doi.org/10.1088/2053-1591/ab66ea>.
- [46] X. Hu, Y. Li, Y. Xu, Z. Gan, X. Zou, J. Shi, X. Huang, Green one-step synthesis of carbon quantum dots from orange peel for fluorescent detection of *Escherichia coli* in milk, *Food Chem.* 339 (2021) 127775–127783.

1029 <https://doi.org/10.1016/j.foodchem.2020.127775>.

1030 [47] A. Rana, K. Yadav, S. Jagadevan, A comprehensive review on green synthesis of nature-inspired metal
 1031 nanoparticles: Mechanism, application and toxicity, J. Clean. Prod. 272 (2020) 1228805–122905.
 1032 <https://doi.org/10.1016/j.jclepro.2020.122880>.

1033 [48] S. He, Z. Guo, Y. Zhang, S. Zhang, J. Wang, N. Gu, Biosynthesis of gold nanoparticles using the bacteria
 1034 *Rhodopseudomonas capsulata*, Mater. Lett. 61 (2007) 3984–3987.
 1035 <https://doi.org/10.1016/j.matlet.2007.01.018>.

1036 [49] G.J. Zhou, S.H. Li, Y.C. Zhang, Y.Z. Fu, Biosynthesis of CdS nanoparticles in banana peel extract, J. Nanosci.
 1037 Nanotechnol. 14 (2014) 4437–4442. <https://doi.org/10.1166/jnn.2014.8259>.

1038 [50] S. Begum, M. Ahmaruzzaman, Green synthesis of SnO₂ quantum dots using *Parkia speciosa* Hassk pods
 1039 extract for the evaluation of anti-oxidant and photocatalytic properties, J. Photochem. Photobiol. B Biol. 184
 1040 (2018) 44–53. <https://doi.org/10.1016/j.jphotobiol.2018.04.041>.

1041 [51] H. Rani, S.P. Singh, T.P. Yadav, M.S. Khan, M.I. Ansari, A.K. Singh, In-vitro catalytic, antimicrobial and
 1042 antioxidant activities of bioengineered copper quantum dots using *Mangifera indica* (L.) leaf extract, Mater.
 1043 Chem. Phys. 239 (2020) 122052–122065. <https://doi.org/10.1016/j.matchemphys.2019.122052>.

1044 [52] A. Nair, J.T. Haponiuk, S. Thomas, S. Gopi, Natural carbon-based quantum dots and their applications in drug
 1045 delivery: A review, Biomed. Pharmacother. 132 (2020) 110834–110849.
 1046 <https://doi.org/10.1016/j.biopha.2020.110834>.

1047 [53] M. Hasan, I. Ullah, H. Zul, K. Naeem, A. Iqbal, H. Gul, Biological entities as chemical reactors for synthesis
 1048 of nanomaterials: Progress, challenges and future perspective, 8 (2018) 13–28.
 1049 <https://doi.org/10.1016/j.mtchem.2018.02.003>.

1050 [54] E. Imbert, Food waste valorization options: Opportunities from the bioeconomy, Open Agric. 2 (2017) 195–
 1051 204. <https://doi.org/10.1515/opag-2017-0020>.

1052 [55] M. Bilal, H.M.N. Iqbal, Sustainable bioconversion of food waste into high-value products by immobilized
 1053 enzymes to meet bio-economy challenges and opportunities – A review, Food Res. Int. 123 (2019) 226–240.
 1054 <https://doi.org/10.1016/j.foodres.2019.04.066>.

1055 [56] J.S. Gregg, J. Jürgens, M.K. Happel, N. Strøm-Andersen, A.N. Tanner, S. Bolwig, A. Klitkou, Valorization
 1056 of bio-residuals in the food and forestry sectors in support of a circular bioeconomy: A review, J. Clean. Prod.
 1057 267 (2020) 122093–122106. <https://doi.org/10.1016/j.jclepro.2020.122093>.

1058 [57] K.L. Ong, G. Kaur, N. Pensupa, K. Uisan, C.S.K. Lin, Trends in food waste valorization for the production of
 1059 chemicals, materials and fuels: Case study South and Southeast Asia, Bioresour. Technol. 248 (2018) 100–
 1060 112. <https://doi.org/10.1016/j.biortech.2017.06.076>.

1061 [58] Y. Niu, D. Zheng, B. Yao, Z. Cai, Z. Zhao, S. Wu, P. Cong, D. Yang, A novel bioconversion for value-added
 1062 products from food waste using *Musca domestica*, Waste Manag. 61 (2017) 455–460.
 1063 <https://doi.org/10.1016/j.wasman.2016.10.054>.

1064 [59] B. Satari, K. Karimi, *Citrus* processing wastes: Environmental impacts, recent advances, and future
 1065 perspectives in total valorization, Resour. Conserv. Recycl. 129 (2018) 153–167.

1066 <https://doi.org/10.1016/j.resconrec.2017.10.032>.

1067 [60] M.A. Farag, B. Abib, L. Ayad, A.R. Khattab, Sweet and bitter oranges: An updated comparative review of
 1068 their bioactives, nutrition, food quality, therapeutic merits and biowaste valorization practices, Food Chem.
 1069 331 (2020) 127306–127319. <https://doi.org/10.1016/j.foodchem.2020.127306>.

1070 [61] B. Song, R. Lin, C.H. Lam, H. Wu, T.H. Tsui, Y. Yu, Recent advances and challenges of inter-disciplinary
 1071 biomass valorization by integrating hydrothermal and biological techniques, Renew. Sustain. Energy Rev. 135
 1072 (2021) 110370–110389. <https://doi.org/10.1016/j.rser.2020.110370>.

1073 [62] B. Shanmugarajah, I.M.L. Chew, N.M. Mubarak, T.S.Y. Choong, C.K. Yoo, K.W. Tan, Valorization of palm
 1074 oil agro-waste into cellulose biosorbents for highly effective textile effluent remediation, J. Clean. Prod. 210
 1075 (2019) 697–709. <https://doi.org/10.1016/j.jclepro.2018.10.342>.

1076 [63] N. Mahato, K. Sharma, M. Sinha, E.R. Baral, R. Koteswararao, A. Dhyani, M. Hwan Cho, S. Cho, Bio-
 1077 sorbents, industrially important chemicals and novel materials from *Citrus* processing waste as a sustainable
 1078 and renewable bioresource: A review, J. Adv. Res. 23 (2020) 61–82.
 1079 <https://doi.org/10.1016/j.jare.2020.01.007>.

1080 [64] M. Nayak, D.K. Swain, R. Sen, Strategic valorization of de-oiled microalgal biomass waste as biofertilizer
 1081 for sustainable and improved agriculture of rice (*Oryza sativa* L.) crop, Sci. Total Environ. 682 (2019) 475–
 1082 484. <https://doi.org/10.1016/j.scitotenv.2019.05.123>.

1083 [65] A. Ibn Ferjani, M. Jeguirim, S. Jellali, L. Limousy, C. Courson, H. Akrou, N. Thevenin, L. Ruidavets, A.
 1084 Muller, S. Bennici, The use of exhausted grape marc to produce biofuels and biofertilizers: Effect of pyrolysis
 1085 temperatures on biochars properties, Renew. Sustain. Energy Rev. 107 (2019) 425–433.
 1086 <https://doi.org/10.1016/j.rser.2019.03.034>.

1087 [66] R. Kapoor, P. Ghosh, M. Kumar, S. Sengupta, A. Gupta, S.S. Kumar, V. Vijay, V. Kumar, V. Kumar Vijay,
 1088 D. Pant, Valorization of agricultural waste for biogas based circular economy in India: A research outlook,
 1089 Bioresour. Technol. 304 (2020) 123036–123047. <https://doi.org/10.1016/j.biortech.2020.123036>.

1090 [67] P. Samaddar, Y. Sik, K. Kim, E.E. Kwon, D.C.W. Tsang, Synthesis of nanomaterials from various wastes and
 1091 their new age applications, J. Clean. Prod. 197 (2018) 1190–1209.
 1092 <https://doi.org/10.1016/j.jclepro.2018.06.262>.

1093 [68] B.A. Omran, O. Aboelazayem, H.N. Nassar, R.A. El-Salamony, N.S. El-Gendy, Biovalorization of mandarin
 1094 waste peels into silver nanoparticles and activated carbon, Int. J. Environ. Sci. Technol. (2020),
 1095 <https://doi.org/10.1007/s13762-020-02873-z>.

1096 [69] M. Wang, R. Shi, M. Gao, K. Zhang, L. Deng, Q. Fu, L. Wang, D. Gao, Sensitivity fluorescent switching
 1097 sensor for Cr (VI) and ascorbic acid detection based on orange peels-derived carbon dots modified with
 1098 EDTA, Food Chem. 318 (2020) 126506–126517. <https://doi.org/10.1016/j.foodchem.2020.126506>.

1099 [70] K.K. Gudimella, T. Appidi, H.F. Wu, V. Battula, A. Jogdand, A.K. Rengan, G. Gedda, Sand bath assisted
 1100 green synthesis of carbon dots from *Citrus* fruit peels for free radical scavenging and cell imaging, Colloids
 1101 Surf. B Biointerfaces. 197 (2021) 111362–11169. <https://doi.org/10.1016/j.colsurfb.2020.111362>.

1102 [71] O. V. Kharissova, B.I. Kharisov, C.M.O. González, Y.P. Méndez, I. López, Greener synthesis of chemical

compounds and materials, R. Soc. open sci. 6 (2019) 191378–191419. <https://doi.org/10.1098/rsos.191378>.

[72] S.L. D'souza, S.S. Chettiar, J.R. Koduru, S.K. Kailasa, Synthesis of fluorescent carbon dots using *Daucus carota* subsp. *sativus* roots for mitomycin drug delivery, Optik 158 (2018) 893–900. <https://doi.org/10.1016/j.ijleo.2017.12.200>.

[73] W. Chen, J. Shen, G. Lv, D. Li, Y. Hu, C. Zhou, X. Liu, Z. Dai, Green synthesis of graphene quantum dots from cotton cellulose, ChemistrySelect. 4 (2019) 2898–2902. <https://doi.org/10.1002/slct.201803512>.

[74] S. Iravani, R.S. Varma, Green synthesis, biomedical and biotechnological applications of carbon and graphene quantum dots. A review, Environ. Chem. Lett. 18 (2020) 703–727. <https://doi.org/10.1007/s10311-020-00984-0>.

[75] N. Murugan, M. Prakash, M. Jayakumar, A. Sundaramurthy, A.K. Sundramoorthy, Green synthesis of fluorescent carbon quantum dots from *Eleusine coracana* and their application as a fluorescence ‘turn-off’ sensor probe for selective detection of Cu^{2+} , Appl. Surf. Sci. 476 (2019) 468–480. <https://doi.org/10.1016/j.apsusc.2019.01.090>.

[76] S. Iravani, R.S. Varma, Plant-derived edible nanoparticles and miRNAs: Emerging frontier for therapeutics and targeted drug-delivery, ACS Sustain. Chem. Eng. 7 (2019) 8055–8069. <https://doi.org/10.1021/acssuschemeng.9b00954>.

[77] Y. Feng, K.E. Marusak, L. You, S. Zauscher, Biosynthetic transition metal chalcogenide semiconductor nanoparticles: Progress in synthesis, property control and applications, Curr. Opin. Colloid Interface Sci. 38 (2018) 190–203. <https://doi.org/10.1016/j.cocis.2018.11.002>.

[78] A. Fernando, K.L.D.M. Weerawardene, N. V Karimova, C.M. Aikens, Quantum mechanical studies of large metal, metal oxide, and metal chalcogenide nanoparticles and clusters, Chem. Rev. 115 (2015) 6112–6216. <https://doi.org/10.1021/cr500506r>.

[79] B. Bajorowicz, M.P. Kobylański, A. Gołębiewska, J. Nadolna, A. Zaleska-Medynska, A. Malankowska, Quantum dot-decorated semiconductor micro- and nanoparticles: A review of their synthesis, characterization and application in photocatalysis, Adv. Colloid Interface Sci. 256 (2018) 352–372. <https://doi.org/10.1016/j.cis.2018.02.003>.

[80] G. Dong, H. Wang, G. Chen, Q. Pan, J. Qiu, Quantum dot-doped glasses and fibers: Fabrication and optical properties, Front. Mater. 2 (2015) 1–14. <https://doi.org/10.3389/fmats.2015.00013>.

[81] J. Xue, X. Wang, J.H. Jeong, X. Yan, Fabrication, photoluminescence and applications of quantum dots embedded glass ceramics, Chem. Eng. J. 383 (2020) 123082–123115. <https://doi.org/10.1016/j.cej.2019.123082>.

[82] M. Kim, J. Bang, Fabrication of visible-light sensitized ZnTe/ZnSe (Core/Shell) type-II quantum dots, J. Korean Ceram. Soc. 55 (2018) 510–514. <https://doi.org/10.4191/kcers.2018.55.5.11>.

[83] J. J. Xue, X. Wang, J. Hyun, X. Yan, Fabrication, photoluminescence and applications of quantum dots embedded glass ceramics, Chem. Eng. J. 383 (2020) 123082–123115. <https://doi.org/10.1016/j.cej.2019.123082>.

[84] J.W. Kyobe, E.B. Mubofu, Y.M.M. Makame, S. Mlowe, N. Revaprasadu, Cadmium sulfide quantum dots

- stabilized by castor oil and ricinoleic acid, Phys. E Low-Dimensional Syst. Nanostructures. 76 (2016) 95–102. <https://doi.org/10.1016/j.physe.2015.10.008>.
- [85] S.R. Bera, S. Saha, Biosynthesis and characterization of *Thevetia peruviana* leaf extract capped CdTe nanoparticles in photoconductive and photovoltaic applications, Mater. Today Proc. 5 (2018) 3476–3485. <https://doi.org/10.1016/j.matpr.2017.11.594>.
- [86] Z. Moradi Alvand, H.R. Rajabi, A. Mirzaei, A. Masoumiasl, H. Sadatfaraji, Rapid and green synthesis of cadmium telluride quantum dots with low toxicity based on a plant-mediated approach after microwave and ultrasonic assisted extraction: Synthesis, characterization, biological potentials and comparison study, Mater. Sci. Eng. C. 98 (2019) 535–544. <https://doi.org/10.1016/j.msec.2019.01.010>.
- [87] H. Yang, C. Liu, D. Yang, H. Zhang, Z. Xi, Comparative study of cytotoxicity, oxidative stress and genotoxicity induced by four typical nanomaterials: The role of particle size, shape and composition, J. Appl. Toxicol. 29 (2009) 69–78. <https://doi.org/10.1002/jat.1385>.
- [88] Y. Yamakoshi, N. Umezawa, A. Ryu, K. Arakane, N. Miyata, Y. Goda, T. Masumizu, T. Nagano, Active oxygen species generated from photoexcited fullerene (C₆₀) as potential medicines: O₂^{•−} versus ¹O₂, J. Am. Chem. Soc. 125 (2003) 12803–12809. <https://doi.org/10.1021/ja0355574>.
- [89] J. Gabbay, G. Borkow, J. Mishal, E. Magen, R. Zatzoff, Y. Shemer-Avni, Copper oxide impregnated textiles with potent biocidal activities, J. Ind. Text. 35 (2006) 323–335. <https://journals.sagepub.com/home/jit>.
- [90] M.S. Meikhail, A.M. Abdelghany, W.M. Awad, Role of CdSe quantum dots in the structure and antibacterial activity of chitosan/poly ε-caprolactone thin films, Egypt. J. Basic Appl. Sci. 5 (2018) 138–144. <https://doi.org/10.1016/j.ejbas.2018.05.003>.
- [91] A.R. Khezripour, D. Souri, H. Tavafi, M. Ghabooli, Serial dilution bioassay for the detection of antibacterial potential of ZnSe quantum dots and their Fourier transform infra-red spectroscopy, Meas. J. Int. Meas. Confed. 148 (2019) 106939–106947. <https://doi.org/10.1016/j.measurement.2019.106939>.
- [92] I.M. Ali, I.M. Ibrahim, E.F. Ahmed, Q.A. Abbas, Structural and characteristics of manganese doped zinc sulfide nanoparticles and its antibacterial effect against Gram-positive and Gram-negative bacteria, Open J. Biophys. 06 (2016) 1–9. <https://doi.org/10.4236/ojbiphy.2016.61001>.
- [93] C. Chaliha, B.K. Nath, P.K. Verma, E. Kalita, Synthesis of functionalized Cu:ZnS nanosystems and its antibacterial potential, Arab. J. Chem. 12 (2019) 515–524. <https://doi.org/10.1016/j.arabjc.2016.05.002>.
- [94] A.K. Singh, P. Pal, V. Gupta, T.P. Yadav, V. Gupta, S.P. Singh, Green synthesis, characterization and antimicrobial activity of zinc oxide quantum dots using *Eclipta alba*, Mater. Chem. Phys. 203 (2018) 40–48.
- [95] D. Baruah, R. Narayan, S. Yadav, A. Yadav, A. Moni, Biology *Alpinia nigra* fruits mediated synthesis of silver nanoparticles and their antimicrobial and photocatalytic activities, J. Photochem. Photobiol. B Biol. 201 (2019) 111649–111658. <https://doi.org/10.1016/j.jphotobiol.2019.111649>.
- [96] I.P. Mukha, A.M. Eremenko, N.P. Smirnova, A.I. Mikhienkova, G.I. Korchak, V.F. Gorchev, A.Y. Chunikhin, Antimicrobial activity of stable silver nanoparticles of a certain size, Appl. Biochem. Microbiol. 49 (2013) 199–206.
- [97] Z. Gholami, M. Dadmehr, N.B. Jelodar, M. Hosseini, A.P. Parizi, One-pot biosynthesis of CdS quantum dots

- through in vitro regeneration of hairy roots of *Rhaphanus sativus* L. And their apoptosis effect on MCF-7 and AGS cancerous human cell lines, Mater. Res. Express. 7 (2020) 15056–15067. <https://doi.org/10.1088/2053-1591/ab66ea>.
- [98] D. Mohanta, M. Ahmaruzzaman, Biogenic synthesis of SnO₂ quantum dots encapsulated carbon nanoflakes: An efficient integrated photocatalytic adsorbent for the removal of bisphenol A from aqueous solution, J. Alloys Compd. 828 (2020) 154093–154103. <https://doi.org/10.1016/j.jallcom.2020.154093>.
- [99] D. Mohanta, M. Ahmaruzzaman, Tin oxide nanostructured materials: An overview of recent developments in synthesis, modifications and potential applications, RSC Adv. 6 (2016) 110996–111015. <https://doi.org/10.1039/C6RA21444D>.
- [100] I. Fatimah, I. Sahroni, O. Muraza, R. Doong, One-pot biosynthesis of SnO₂ quantum dots mediated by *Clitoria ternatea* flower extract for photocatalytic degradation of rhodamine B, J. Environ. Chem. Eng. 8 (2020) 103879–103891. <https://doi.org/10.1016/j.jece.2020.103879>.
- [101] G. Bhuvaneswari, S. Radjarejesri, Green Synthesis and Characterization of CdS Quantum Dots, 8 (2015) 104–108.
- [102] A. Mahalakshmi, G. Baskar, Green Synthesis and characterization of cadmium-tellurium quantum dots using pomelo peel aqueous extract, J. Electron. Mater. 48 (2019) 5975–5979. <https://doi.org/10.1007/s11664-019-07352-x>.
- [103] R. Lakshmi pathy, N.C. Sarada, K. Chidambaram, S.K. Pasha, One-step, low-temperature fabrication of CdS quantum dots by watermelon rind: A green approach, Int. J. Nanomedicine. 10 (2015) 183–188. <https://doi.org/10.2147/IJN.S79988>.
- [104] K. Kandasamy, M. Venkatesh, Y.A. Syed Khadar, P. Rajasingh, One-pot green synthesis of CdS quantum dots using *Opuntia ficus-indica* fruit sap, Mater. Today Proc. 26 (2019) 3503–3506. <https://doi.org/10.1016/j.matpr.2019.06.003>.
- [105] L. Guo, L. Li, M. Liu, Q. Wan, J. Tian, Q. Huang, Y. Wen, S. Liang, X. Zhang, Y. Wei, Bottom-up preparation of nitrogen doped carbon quantum dots with green emission under microwave-assisted hydrothermal treatment and their biological imaging, Mater. Sci. Eng. C. 84 (2018) 60–66. <https://doi.org/10.1016/j.msec.2017.11.034>.
- [106] C. Shi, H. Qi, R. Ma, Z. Sun, L. Xiao, G. Wei, Z. Huang, S. Liu, J. Li, M. Dong, J. Fan, Z. Guo, N,S-self-doped carbon quantum dots from fungus fibers for sensing tetracyclines and for bioimaging cancer cells, Mater. Sci. Eng. C. 105 (2019) 110132–110140. <https://doi.org/10.1016/j.msec.2019.110132>.
- [107] X. Xu, R. Ray, Y. Gu, H.J. Ploehn, L. Gearheart, K. Raker, W.A. Scrivens, Electrophoretic analysis and purification of fluorescent single-walled carbon nanotube fragments, J. Am. Chem. Soc. 126 (2004) 12736–12737. <https://doi.org/10.1021/ja040082h>.
- [108] N. Tejwan, S.K. Saha, J. Das, Multifaceted applications of green carbon dots synthesized from renewable sources, Adv. Colloid Interface Sci. 275 (2020) 102046–102064. <https://doi.org/10.1016/j.cis.2019.102046>.
- [109] Y.-P. Sun, B. Zhou, Y. Lin, W. Wang, K.A.S. Fernando, P. Pathak, M.J. Meziani, B.A. Harruff, X. Wang, H. Wang, Quantum-sized carbon dots for bright and colorful photoluminescence, J. Am. Chem. Soc. 128 (2006)

7756–7757. <https://doi.org/10.1021/ja062677d>.

[110] K. Ken, C. Stephanie, H. Kit, Y.K. Yong, Biogreen Synthesis of Carbon Dots for Biotechnology and Nanomedicine Applications, Springer Berlin Heidelberg, 2018. <https://doi.org/10.1007/s40820-018-0223-3>.

[111] X. Nie, S. Wu, A. Mensah, K. Lu, Q. Wei, Carbon quantum dots embedded electrospun nanofibers for efficient antibacterial photodynamic inactivation, Mater. Sci. Eng. C. 108 (2020) 110377–110388. <https://doi.org/10.1016/j.msec.2019.110377>.

[112] M. Lu, L. Zhou, One-step sonochemical synthesis of versatile nitrogen-doped carbon quantum dots for sensitive detection of Fe²⁺ ions and temperature in vitro, Mater. Sci. Eng. C. 101 (2019) 352–359. <https://doi.org/10.1016/j.msec.2019.03.109>.

[113] V. Sharma, P. Tiwari, S.M. Mobin, Sustainable carbon-dots: Recent advances in green carbon dots for sensing and bioimaging, J. Mater. Chem. B. 5 (2017) 8904–8924. <https://doi.org/10.1039/C7TB02484C>.

[114] M. Ashra, R. Mohammadinejad, S. Kumar, Z. Ahmadi, E. Ghasemipour, A. Pardakhty, Carbon dots as versatile nanoarchitectures for the treatment of neurological disorders and their theranostic applications: A review, 278 (2020) 1–12. <https://doi.org/10.1016/j.cis.2020.102123>.

[115] Y. Liu, Y. Zhao, Y. Zhang, One-step green synthesized fluorescent carbon nanodots from bamboo leaves for copper(II) ion detection, Sensors Actuators, B Chem. 196 (2014) 647–652. <https://doi.org/10.1016/j.snb.2014.02.053>.

[116] S. Gao, Y. Chen, H. Fan, X. Wei, C. Hu, L. Wang, L. Qu, A green one-arrow-two-hawks strategy for nitrogen-doped carbon dots as fluorescent ink and oxygen reduction electrocatalysts, J. Mater. Chem. A. 2 (2014) 6320–6325. <https://doi.org/10.1039/c3ta15443b>.

[117] A. Sachdev, P. Gopinath, Green synthesis of multifunctional carbon dots from coriander leaves and their potential application as antioxidants, sensors and bioimaging agents, Analyst. 140 (2015) 4260–4269. <https://doi.org/10.1039/c5an00454c>.

[118] N. Sarkar, G. Sahoo, R. Das, G. Prusty, S.K. Swain, Carbon quantum dot tailored calcium alginate hydrogel for pH responsive controlled delivery of vancomycin, Eur. J. Pharm. Sci. 109 (2017) 359–371. <https://doi.org/10.1016/j.ejps.2017.08.015>.

[119] T. Kavitha, S. Kumar, Turning date palm fronds into biocompatible mesoporous fluorescent carbon dots, Sci. Rep. 8 (2018) 1–10. <https://doi.org/10.1038/s41598-018-34349-z>.

[120] X. Jiang, D. Qin, G. Mo, J. Feng, C. Yu, W. Mo, Analysis Ginkgo leaf-based synthesis of nitrogen-doped carbon quantum dots for highly sensitive detection of salazosulfapyridine in mouse plasma, J. Pharm. Biomed. Anal. 164 (2019) 514–519. <https://doi.org/10.1016/j.jpba.2018.11.025>.

[121] T. Arumugham, M. Alagumuthu, R.G. Amimodu, S. Munusamy, S.K. Iyer, A sustainable synthesis of green carbon quantum dot (CQD) from *Catharanthus roseus* (white flowering plant) leaves and investigation of its dual fluorescence responsive behavior in multi-ion detection and biological applications, Sustain. Mater. Technol. 23 (2020) e00138–e00149. <https://doi.org/10.1016/j.susmat.2019.e00138>.

[122] D. Bano, V. Kumar, V.K. Singh, S.H. Hasan, Green synthesis of fluorescent carbon quantum dots for the detection of mercury (ii) and glutathione, New J. Chem. 42 (2018) 5814–5821.

1251 <https://doi.org/10.1039/c8nj00432c>.

1252 [123] J. Zhou, Z. Sheng, H. Han, M. Zou, C. Li, Facile synthesis of fluorescent carbon dots using watermelon peel

1253 as a carbon source, *Mater. Lett.* 66 (2012) 222–224. <https://doi.org/10.1016/j.matlet.2011.08.081>.

1254 [124] W. Lu, X. Qin, S. Liu, G. Chang, Y. Zhang, Y. Luo, A.M. Asiri, A.O. Al-Youbi, X. Sun, Economical, green

1255 synthesis of fluorescent carbon nanoparticles and their use as probes for sensitive and selective detection of

1256 mercury(II) ions, *Anal. Chem.* 84 (2012) 5351–5357. <https://doi.org/10.1021/ac3007939>.

1257 [125] A. Prasannan, T. Imae, One-pot synthesis of fluorescent carbon dots from orange waste peels, *Ind. Eng. Chem.*

1258 *Res.* 52 (2013) 15673–15678. <https://doi.org/10.1021/ie402421s>.

1259 [126] R. Bandi, B.R. Gangapuram, R. Dadigala, R. Eslavath, S.S. Singh, V. Guttena, Facile and green synthesis of

1260 fluorescent carbon dots from onion waste and their potential applications as sensor and multicolour imaging

1261 agents, *RSC Adv.* 6 (2016) 28633–28639. <https://doi.org/10.1039/c6ra01669c>.

1262 [127] T. Chatzimitakos, A. Kasouni, L. Sygellou, A. Avgeropoulos, A. Troganis, C. Stalikas, Two of a kind but

1263 different: Luminescent carbon quantum dots from *Citrus* peels for iron and tartrazine sensing and cell imaging,

1264 *Talanta.* 175 (2017) 305–312. <https://doi.org/10.1016/j.talanta.2017.07.053>.

1265 [128] P. Xiao, Y. Ke, J. Lu, Z. Huang, X. Zhu, B. Wei, L. Huang, Photoluminescence immunoassay based on

1266 grapefruit peel-extracted carbon quantum dots encapsulated into silica nanospheres for p53 protein, *Biochem.*

1267 *Eng. J.* 139 (2018) 109–116. <https://doi.org/10.1016/j.bej.2018.08.012>.

1268 [129] S.A.A. Vandarkuzhali, S. Natarajan, S. Jeyabalan, G. Sivaraman, S. Singaravadivel, S. Muthusubramanian,

1269 B. Viswanathan, Pineapple peel-derived carbon dots: Applications as sensor, molecular keypad lock, and

1270 memory device, *ACS Omega.* 3 (2018) 12584–12592. <https://doi.org/10.1021/acsomega.8b01146>.

1271 [130] S. Ghosh, K. Ghosal, S.A. Mohammad, K. Sarkar, Dendrimer functionalized carbon quantum dot for selective

1272 detection of breast cancer and gene therapy, *Chem. Eng. J.* 373 (2019) 468–484.

1273 <https://doi.org/10.1016/j.cej.2019.05.023>.

1274 [131] X.Y. Jiao, L. shuang Li, S. Qin, Y. Zhang, K. Huang, L. Xu, The synthesis of fluorescent carbon dots from

1275 mango peel and their multiple applications, *Colloids Surfaces A Physicochem. Eng. Asp.* 577 (2019) 306–

1276 314. <https://doi.org/10.1016/j.colsurfa.2019.05.073>.

1277 [132] S.A.A. Vandarkuzhali, V. Jeyalakshmi, G. Sivaraman, S. Singaravadivel, K.R. Krishnamurthy, B.

1278 Viswanathan, Highly fluorescent carbon dots from pseudo-stem of banana plant: Applications as nanosensor

1279 and bio-imaging agents, *Sensors Actuators, B Chem.* 252 (2017) 894–900.

1280 <https://doi.org/10.1016/j.snb.2017.06.088>.

1281 [133] D. Tang, Y. Lin, Q. Zhou, Carbon dots prepared from *Litchi chinensis* and modified with manganese dioxide

1282 nanosheets for use in a competitive fluorometric immunoassay for aflatoxin B1, *Microchim. Acta.* 185 (2018)

1283 1–9. <https://doi.org/10.1007/s00604-018-3012-2>.

1284 [134] A. Kumar, A.R. Chowdhuri, D. Laha, T.K. Mahto, P. Karmakar, S.K. Sahu, Green synthesis of carbon dots

1285 from *Ocimum sanctum* for effective fluorescent sensing of Pb²⁺ ions and live cell imaging, *Sensors Actuators,*

1286 *B Chem.* 242 (2017) 679–686. <https://doi.org/10.1016/j.snb.2016.11.109>.

1287 [135] S. Bhatt, M. Bhatt, A. Kumar, G. Vyas, T. Gajaria, P. Paul, Green route for synthesis of multifunctional

- fluorescent carbon dots from Tulsi leaves and its application as Cr(VI) sensors, bio-imaging and patterning agents, *Colloids Surf. B Biointerfaces*. 167 (2018) 126–133. <https://doi.org/10.1016/j.colsurfb.2018.04.008>.
- [136] M. Asha Jhonsi, A. Kathiravan, Photoinduced interaction of arylamine dye with carbon quantum dots ensued from *Centella asiatica*, *J. Lumin.* 192 (2017) 321–327. <https://doi.org/10.1016/j.jlumin.2017.06.056>.
- [137] M. Shahshahanipour, B. Rezaei, A.A. Ensafi, Z. Etemadifar, An ancient plant for the synthesis of a novel carbon dot and its applications as an antibacterial agent and probe for sensing of an anti-cancer drug, *Mater. Sci. Eng. C*. 98 (2019) 826–833. <https://doi.org/10.1016/j.msec.2019.01.041>.
- [138] N. Kaur, V. Sharma, P. Tiwari, A.K. Saini, S.M. Mobin, “*Vigna radiata*” based green C-dots: Photo-triggered theranostics, fluorescent sensor for extracellular and intracellular iron (III) and multicolor live cell imaging probe, *Sensors Actuators, B Chem.* 291 (2019) 275–286. <https://doi.org/10.1016/j.snb.2019.04.039>.
- [139] N. Pourreza, M. Ghomi, Green synthesized carbon quantum dots from *Prosopis juliflora* leaves as a dual off-on fluorescence probe for sensing mercury (II) and chemet drug, *Mater. Sci. Eng. C*. 98 (2019) 887–896. <https://doi.org/10.1016/j.msec.2018.12.141>.
- [140] L. Komalavalli, P. Amutha, S. Monisha, A facile approach for the synthesis of carbon dots from *Hibiscus sabdariffa* & its application as bio-imaging agent and Cr (VI) sensor, *Mater. Today Proc.* (2020), <https://doi.org/10.1016/j.matpr.2020.04.195>.
- [141] S. Raina, A. Thakur, A. Sharma, D. Pooja, A.P. Minhas, Bactericidal activity of *Cannabis sativa* phytochemicals from leaf extract and their derived carbon dots and Ag@carbon dots, *Mater. Lett.* 262 (2020) 127122–127127. <https://doi.org/10.1016/j.matlet.2019.127122>.
- [142] B. Sun, F. Wu, Q. Zhang, X. Chu, Z. Wang, X. Huang, J. Li, C. Yao, N. Zhou, J. Shen, Insight into the effect of particle size distribution differences on the antibacterial activity of carbon dots, *J. Colloid Interface Sci.* 584 (2021) 505–519. <https://doi.org/10.1016/j.jcis.2020.10.015>.
- [143] H.-J. Jian, R.-S. Wu, T.-Y. Lin, Y.-J. Li, H.-J. Lin, S.G. Harroun, J.-Y. Lai, C.-C. Huang, Super-cationic carbon quantum dots synthesized from spermidine as an eye drop formulation for topical treatment of bacterial keratitis, *ACS Nano*. 11 (2017) 6703–6716. <https://doi.org/10.1021/acsnano.7b01023>.
- [144] L. Hui, J. Huang, G. Chen, Y. Zhu, L. Yang, Antibacterial property of graphene quantum dots (both source material and bacterial shape matter), *ACS Appl. Mater. Interfaces*. 8 (2016) 20–25. <https://doi.org/10.1021/acsami.5b10132>.
- [145] N.A. Travlou, M. Algarra, C. Alcoholado, M. Cifuentes-rueda, E. Rodr, A.M. Labella, J. Manuel, T.J. Badosz, Carbon Quantum dot surface-chemistry-dependent Ag release governs the high antibacterial activity of Ag-metal–organic framework composites, *ACS Appl. Bio Mater.* 1 (2018) 693–707. <https://doi.org/10.1021/acsabm.8b00166>.
- [146] J. Singh, S. Kaur, J. Lee, A. Mehta, S. Kumar, K. Kim, S. Basu, M. Rawat, Highly fluorescent carbon dots derived from *Mangifera indica* leaves for selective detection of metal ions, *Sci. Total Environ.* 720 (2020) 137604–137612. <https://doi.org/10.1016/j.scitotenv.2020.137604>.
- [147] R. Dineshkumar, S. Devikala, Facile synthesis of fluorescent carbon quantum dots from Betel leafs (*Piper betle*) for Fe³⁺ sensing, *Mater. Today Proc.* (2020), <https://doi.org/10.1016/j.matpr.2020.03.096>.

- [148] M. Sabet, K. Mahdavi, Green synthesis of high photoluminescence nitrogen-doped carbon quantum dots from grass via a simple hydrothermal method for removing organic and inorganic water pollutions, *Appl. Surf. Sci.* 463 (2019) 283–291. <https://doi.org/10.1016/j.apsusc.2018.08.223>.
- [149] A. Mewada, S. Pandey, S. Shinde, N. Mishra, G. Oza, M. Thakur, M. Sharon, M. Sharon, Green synthesis of biocompatible carbon dots using aqueous extract of *Trapa bispinosa* peel, *Mater. Sci. Eng. C* 33 (2013) 2914–2917. <https://doi.org/10.1016/j.msec.2013.03.018>.
- [150] R. Atchudan, T.N.J.I. Edison, M.G. Sethuraman, Y.R. Lee, Efficient synthesis of highly fluorescent nitrogen-doped carbon dots for cell imaging using unripe fruit extract of *Prunus mume*, *Appl. Surf. Sci.* 384 (2016) 432–441. <https://doi.org/10.1016/j.apsusc.2016.05.054>.
- [151] J. Ma, H. Yu, X. Jiang, Z. Luo, Y. Zheng, High sensitivity label-free detection of Fe^{3+} ion in aqueous solution using fluorescent MoS_2 quantum dots, *Sensors Actuators B. Chem.* 281 (2019) 989–997. <https://doi.org/10.1016/j.snb.2018.11.039>.
- [152] X. Bao, X. Cao, X. Nie, Y. Xu, W. Guo, B. Zhou, A new selective fluorescent chemical sensor for Fe^{3+} based on conjugate and its imaging in living cells, *Sensors Actuators B. Chem.* 208 (2015) 54–66. <https://doi.org/10.1016/j.snb.2014.10.127>.
- [153] C. Wang, H. Shi, M. Yang, Y. Yan, E. Liu, Z. Ji, J. Fan, Facile synthesis of novel carbon quantum dots from biomass waste for highly sensitive detection of iron ions, *Mater. Res. Bull.* 124 (2020) 110730–110738. <https://doi.org/10.1016/j.materresbull.2019.110730>.
- [154] T.N.J.I. Edison, R. Atchudan, N. Karthik, J. Balaji, D. Xiong, Y.R. Lee, Catalytic degradation of organic dyes using green synthesized N-doped carbon supported silver nanoparticles, *Fuel* 280 (2020) 118682–118689. <https://doi.org/10.1016/j.fuel.2020.118682>.
- [155] H. Muktha, R. Sharath, N. Kottam, Green Synthesis of carbon dots and evaluation of its pharmacological activities, *BioNanoScience* 10 (2020) 731–44. <https://doi.org/10.1007/s12668-020-00741-1>.
- [156] V. V. Makarov, A.J. Love, O. V. Sinitsyna, S.S. Makarova, I. V. Yaminsky, M.E. Taliansky, N.O. Kalinina, “Green” nanotechnologies: synthesis of metal nanoparticles using plants, *Acta Naturae* 6 (2014) 35–44.
- [157] K. Shah, J.M. Nongkynrih, Metal hyperaccumulation and bioremediation, *Biol. Plant.* 51 (2007) 618–634. <https://doi.org/10.1007/s10535-007-0134-5>.
- [158] S. Michalet, S. Rouifed, T. Pellassa-Simon, M. Fusade-Boyer, G. Meiffren, S. Nazaret, F. Piola, Tolerance of Japanese knotweed *s.l.* to soil artificial polymetallic pollution: early metabolic responses and performance during vegetative multiplication, *Environ. Sci. Pollut. Res.* 24 (2017) 20897–20907. DOI 10.1007/s11356-017-9716-8.
- [159] H. Balafrej, D. Bogusz, Z. El Abidine Triqui, A. Guedira, N. Bendaou, A. Smouni, M. Fahr, Zinc hyperaccumulation in plants: A review, *Plants* 9 (2020) 562–584. <https://doi.org/10.3390/plants9050562>.
- [160] P. Filippou, P. Bouchagier, E. Skotti, V. Fotopoulos, Proline and reactive oxygen/nitrogen species metabolism is involved in the tolerant response of the invasive plant species *Ailanthus altissima* to drought and salinity, *Environ. Exp. Bot.* 97 (2014) 1–10. <https://doi.org/10.1016/j.envexpbot.2013.09.010>.
- [161] W.H.T. Ting, I.A.W. Tan, S.F. Salleh, N.A. Wahab, Application of water hyacinth (*Eichhornia crassipes*) for

1362 phytoremediation of ammoniacal nitrogen: A review, J. Water Process Eng. 22 (2018) 239–249.
 1363 <https://doi.org/10.1016/j.jwpe.2018.02.011>.

1364 [162] H. Ali, E. Khan, M. Anwar, Phytoremediation of heavy metals — Concepts and applications, Chemosphere
 1365 91 (2013) 869–881. <https://doi.org/10.1016/j.chemosphere.2013.01.075>.

1366 [163] B. Leitenmaier, H. Küpper, Cadmium uptake and sequestration kinetics in individual leaf cell protoplasts of
 1367 the Cd/Zn hyperaccumulator *Thlaspi caerulescens*, Plant. Cell Environ. 34 (2011) 208–219.
 1368 <https://doi.org/10.1111/j.1365-3040.2010.02236.x>.

1369 [164] Z. Mashwani, M. Ali, T. Khan, A. Nadhman, Applications of plant terpenoids in the synthesis of colloidal
 1370 silver nanoparticles, Adv. Colloid Interface Sci. 234 (2016) 132–141.
 1371 <https://doi.org/10.1016/j.cis.2016.04.008>.

1372 [165] N. Ahmad, S. Sharma, M.K. Alam, V.N. Singh, S.F. Shamsi, B.R. Mehta, A. Fatma, Rapid synthesis of silver
 1373 nanoparticles using dried medicinal plant of basil, Colloids Surf. B Biointerfaces 81 (2010) 81–86.
 1374 <https://doi.org/10.1016/j.colsurfb.2010.06.029>.

1375 [166] S. Mandal, P.R. Selvakannan, S. Phadtare, R. Pasricha, M. Sastry, Synthesis of a stable gold hydrosol by the
 1376 reduction of chloroaurate ions by the amino acid, aspartic acid, J. Chem. Sci. 114 (2002) 513–520.
 1377 <https://doi.org/10.1007/BF02704195>.

1378 [167] S. Panigrahi, S. Kundu, S. Ghosh, S. Nath, T. Pal, General method of synthesis for metal nanoparticles, J.
 1379 Nanoparticle Res. 6 (2004) 411–414. <https://doi.org/10.1007/s11051-004-6575-2>.

1380 [168] R. Bandi, R. Dadigala, B.R. Gangapuram, V. Guttena, Green synthesis of highly fluorescent nitrogen – doped
 1381 carbon dots from *Lantana camara* berries for effective detection of lead(II) and bioimaging, J. Photochem.
 1382 Photobiol. B Biol. 178 (2018) 330–338. <https://doi.org/10.1016/j.jphotobiol.2017.11.010>.

1383 [169] M.A. Nasser, H. Keshtkar, M. Kazemnejadi, A. Allahresani, Phytochemical properties and antioxidant
 1384 activity of *Echinops persicus* plant extract: Green synthesis of carbon quantum dots from the plant extract, SN
 1385 Appl. Sci. 2 (2020) 1–12. <https://doi.org/10.1007/s42452-020-2466-0>.

1386 [170] M. Asha Jhonsi, A. Kathiravan, Photoinduced interaction of arylamine dye with carbon quantum dots ensued
 1387 from *Centella asiatica*, J. Lumin. 192 (2017) 321–327. <https://doi.org/10.1016/j.jlumin.2017.06.056>.

1388 [171] X. Zhao, S. Liao, L. Wang, Q. Liu, X. Chen, Facile green and one-pot synthesis of *Purple perilla* derived
 1389 carbon quantum dot as a fluorescent sensor for silver ion, Talanta. 201 (2019) 1–8.
 1390 <https://doi.org/10.1016/j.talanta.2019.03.095>.

1391 [172] Q. Yang, J. Duan, W. Yang, X. Li, J. Mo, P. Yang, Q. Tang, Nitrogen-doped carbon quantum dots from
 1392 biomass via simple one-pot method and exploration of their application, Appl. Surf. Sci. 434 (2018) 1079–
 1393 1085. <https://doi.org/10.1016/j.apsusc.2017.11.040>.

1394 [173] S. Bayda, M. Hadla, S. Palazzolo, V. Kumar, I. Caligiuri, E. Ambrosi, E. Pontoglio, M. Agostini, T.
 1395 Tuccinardi, A. Benedetti, P. Riello, V. Canzonieri, G. Corona, G. Toffoli, F. Rizzolio, Bottom-up synthesis
 1396 of carbon nanoparticles with higher doxorubicin efficacy, J. Control. Release. 248 (2017) 144–152.
 1397 <https://doi.org/10.1016/j.jconrel.2017.01.022>.

1398 [174] K. Doshi, A.A. Mungray, Bio-route synthesis of carbon quantum dots from tulsi leaves and its application as

- a draw solution in forward osmosis, *J. Environ. Chem. Eng.* 8 (2020) 104174–104183. <https://doi.org/10.1016/j.jece.2020.104174>.
- [175] R. Ramanarayanan, S. Swaminathan, Synthesis and characterisation of green luminescent carbon dots from guava leaf extract, *Mater. Today Proc.* 33 (2020) 2223–2227. <https://doi.org/10.1016/j.matpr.2020.03.805>.
- [176] K. Shivaji, M.G. Balasubramanian, A. Devadoss, V. Asokan, C.S. De Castro, M.L. Davies, P. Ponnuragan, S. Pitchaimuthu, Utilization of waste tea leaves as bio-surfactant in CdS quantum dots synthesis and their cytotoxicity effect in breast cancer cells, *Appl. Surf. Sci.* 487 (2019) 159–170. <https://doi.org/10.1016/j.apsusc.2019.05.050>.
- [177] E. Oh, R. Liu, A. Nel, K.B. Gemill, M. Bilal, Y. Cohen, I.L. Medintz, Meta-analysis of cellular toxicity for cadmium-containing quantum dots, *Nat. Nanotechnol.* 11 (2016) 479–494, doi: 10.1038/NNANO.2015.338.
- [178] H. Gao, C.P. Teng, D. Huang, W. Xu, C. Zheng, Y. Chen, M. Liu, D.-P. Yang, M. Lin, Z. Li, Microwave assisted synthesis of luminescent carbonaceous nanoparticles from silk fibroin for bioimaging, *Mater. Sci. Eng. C.* 80 (2017) 616–623. <https://doi.org/10.1016/j.msec.2017.07.007>.
- [179] E. Yaghini, H. Turner, A. Pilling, I. Naasani, A.J. MacRobert, In vivo biodistribution and toxicology studies of cadmium-free indium-based quantum dot nanoparticles in a rat model, *Nanomedicine Nanotechnology, Biol. Med.* 14 (2018) 2644–2655. <https://doi.org/10.1016/j.nano.2018.07.009>.
- [180] T. Pons, E. Pic, N. Lequeux, E. Cassette, L. Bezdetnaya, F. Guillemin, F. Marchal, B. Dubertret, Cadmium-free CuInS₂/ZnS quantum dots for sentinel lymph node imaging with reduced toxicity, *ACS Nano.* 4 (2010) 2531–2538. <https://doi.org/10.1021/nn901421v>.
- [181] Y. Wang, P. Anilkumar, L. Cao, J.-H. Liu, P.G. Luo, K.N. Tackett, S. Sahu, P. Wang, X. Wang, Y.-P. Sun, Carbon dots of different composition and surface functionalization: Cytotoxicity issues relevant to fluorescence cell imaging, *Exp. Biol. Med.* 236 (2011) 1231–1238. <https://doi.org/10.1258%2Febm.2011.011132>.
- [182] M. Havrdova, K. Hola, J. Skopalik, K. Tomankova, M. Petr, K. Cepe, K. Polakova, J. Tucek, A.B. Bourlinos, R. Zboril, Toxicity of carbon dots—Effect of surface functionalization on the cell viability, reactive oxygen species generation and cell cycle, *Carbon N. Y.* 99 (2016) 238–248. <https://doi.org/10.1016/j.carbon.2015.12.027>.
- [183] P. Devi, S. Saini, K. Kim, The advanced role of carbon quantum dots in nanomedical applications, *Biosens. Bioelectron.* 141 (2019) 111158–111175. <https://doi.org/10.1016/j.bios.2019.02.059>.
- [184] J.-H. Park, L. Gu, G. Von Maltzahn, E. Ruoslahti, S.N. Bhatia, M.J. Sailor, Biodegradable luminescent porous silicon nanoparticles for in vivo applications, *Nat. Mater.* 8 (2009) 331–336. DOI: 10.1038/NMAT2398.
- [185] X.T. Zheng, A. Ananthanarayanan, K.Q. Luo, P. Chen, Glowing graphene quantum dots and carbon dots: Properties, syntheses, and biological applications, *Small.* 11 (2015) 1620–1636. <https://doi.org/10.1002/sml.201402648>.
- [186] H.V. Xu, X.T. Zheng, Y. Zhao, Y.N. Tan, Uncovering the design principle of amino acid-derived photoluminescent biodots with tailor-made structure—properties and applications for cellular bioimaging, *ACS Appl. Mater. Interfaces.* 10 (2018) 19881–19888. <https://doi.org/10.1021/acsami.8b04864>.

- [187] S. Kanagasubbulakshmi, I. Gowtham, K. Kadirvelu, K. Archana, Biocompatible methionine-capped CdS/ZnS quantum dots for live cell nucleus imaging, *MRS Commun.* 9 (2019) 344–351. <https://doi.org/10.1557/mrc.2018.238>.
- [188] X.T. Zheng, Y.C. Lai, Y.N. Tan, Nucleotide-derived theranostic nanodots with intrinsic fluorescence and singlet oxygen generation for bioimaging and photodynamic therapy, *Nanoscale Adv.* 1 (2019) 2250–2257. <https://doi.org/10.1039/C9NA00058E>.
- [189] R. Hardman, A toxicologic review of quantum dots: Toxicity depends on physicochemical and environmental factors, *Environ. Health Perspect.* 114 (2006) 165–172. <https://doi.org/10.1289/ehp.8284>.
- [190] C.-H. Lin, M.-H. Yang, L.W. Chang, C.-S. Yang, H. Chang, W.-H. Chang, M.-H. Tsai, C.-J. Wang, P. Lin, Cd/Se/Te-based quantum dot 705 modulated redox homeostasis with hepatotoxicity in mice, *Nanotoxicology* 5 (2011) 650–663. <https://doi.org/10.3109/17435390.2010.539712>.
- [191] Y. Tang, S. Han, H. Liu, X. Chen, L. Huang, X. Li, J. Zhang, The role of surface chemistry in determining in vivo biodistribution and toxicity of CdSe/ZnS core–shell quantum dots, *Biomaterials.* 34 (2013) 8741–8755. <https://doi.org/10.1016/j.biomaterials.2013.07.087>.
- [192] Y. Lu, S. Xu, H. Chen, M. He, Y. Deng, Z. Cao, H. Pi, C. Chen, M. Li, Q. Ma, CdSe/ZnS quantum dots induce hepatocyte pyroptosis and liver inflammation via NLRP3 inflammasome activation, *Biomaterials.* 90 (2016) 27–39. <https://doi.org/10.1016/j.biomaterials.2016.03.003>.
- [193] S. Jha, P. Mathur, S. Ramteke, N.K. Jain, Pharmaceutical potential of quantum dots, *Artif. Cells, Nanomedicine Biotechnol.* 46 (2018) 57–65. <https://doi.org/10.1080/21691401.2017.1411932>.
- [194] K.-T. Yong, W.-C. Law, R. Hu, L. Ye, L. Liu, M.T. Swihart, P.N. Prasad, Nanotoxicity assessment of quantum dots: From cellular to primate studies, *Chem. Soc. Rev.* 42 (2013) 1236–1250. <https://doi.org/10.1039/C2CS35392J>.
- [195] H.E. Pace, E.K. Leshner, J.F. Ranville, Influence of stability on the acute toxicity of CdSe/ZnS nanocrystals to *Daphnia magna*, *Environ. Toxicol. Chem.* 29 (2010) 1338–1344. <https://doi.org/10.1002/etc.168>.
- [196] B. Dubertret, P. Skourides, D.J. Norris, V. Noireaux, A.H. Brivanlou, A. Libchaber, In vivo imaging of quantum dots encapsulated in phospholipid micelles, *Science* 298 (2002) 1759–1762. DOI: 10.1126/science.1077194.
- [197] K.M. Tsoi, Q. Dai, B.A. Alman, W.C.W. Chan, Are quantum dots toxic? Exploring the discrepancy between cell culture and animal studies, *Acc. Chem. Res.* 46 (2013) 662–671. <https://doi.org/10.1021/ar300040z>.
- [198] H.C. Fischer, L. Liu, K.S. Pang, W.C.W. Chan, Pharmacokinetics of nanoscale quantum dots: In vivo distribution, sequestration, and clearance in the rat, *Adv. Funct. Mater.* 16 (2006) 1299–1305. <https://doi.org/10.1002/adfm.200500529>.
- [199] F. Zhao, H. Meng, L. Yan, B. Wang, Y. Zhao, Nanosurface chemistry and dose govern the bioaccumulation and toxicity of carbon nanotubes, metal nanomaterials and quantum dots in vivo, *Sci. Bull.* 60 (2015) 3–20. <https://doi.org/10.1007/s11434-014-0700-0>.
- [200] M. Ashrafizadeh, R. Mohammadinejad, S.K. Kailasa, Z. Ahmadi, E.G. Afshar, A. Pardakhty, Carbon dots as versatile nanoarchitectures for the treatment of neurological disorders and their theranostic applications: A

review, *Adv. Colloid Interface Sci.* 278 (2020) 1–12. <https://doi.org/10.1016/j.cis.2020.102123>.

[201] T. Zhang, Y. Wang, L. Kong, Y. Xue, M. Tang, Threshold dose of three types of quantum dots (QDs) induces oxidative stress triggers DNA damage and apoptosis in mouse fibroblast L929 cells, *Int. J. Environ. Res. Public Health*. 12 (2015) 13435–13454. <https://doi.org/10.3390/ijerph121013435>.

[202] Y. Zhang, Cell toxicity mechanism and biomarker, *Clin. Transl. Med.* 7 (2018) 34–40. <https://doi.org/10.1186/s40169-018-0212-7>.

[203] J. Liu, R. Hu, J. Liu, B. Zhang, Y. Wang, X. Liu, W.C. Law, L. Liu, L. Ye, K.T. Yong, Cytotoxicity assessment of functionalized CdSe, CdTe and InP quantum dots in two human cancer cell models, *Mater. Sci. Eng. C*. 57 (2015) 222–231. <https://doi.org/10.1016/j.msec.2015.07.044>.

[204] B.R. Prasad, N. Nikolskaya, D. Connolly, T.J. Smith, S.J. Byrne, V.A. Gérard, Y.K. Gun'ko, Y. Rochev, Long-term exposure of CdTe quantum dots on PC12 cellular activity and the determination of optimum non-toxic concentrations for biological use, *J. Nanobiotechnology*. 8 (2010) 1–16. <https://doi.org/10.1186/1477-3155-8-7>.

[205] W. Liu, S. Zhang, L. Wang, C. Qu, C. Zhang, L. Hong, L. Yuan, Z. Huang, Z. Wang, S. Liu, CdSe quantum dot (QD)-induced morphological and functional impairments to liver in mice, *PLoS One*. 6 (2011) e24406–e24413. <https://doi.org/10.1371/journal.pone.0024406>.

[206] J. Kim, B.T. Huy, K. Sakthivel, H.J. Choi, W.H. Joo, S.K. Shin, M.J. Lee, Y.I. Lee, Highly fluorescent CdTe quantum dots with reduced cytotoxicity-A Robust biomarker, *Sens. Bio-Sensing Res.* 3 (2015) 46–52. <https://doi.org/10.1016/j.sbsr.2014.12.001>.

[207] T. Zhang, Y. Hu, M. Tang, L. Kong, J. Ying, T. Wu, Y. Xue, Y. Pu, Liver toxicity of cadmium telluride quantum dots (CdTe QDs) due to oxidative stress in vitro and in vivo, *Int. J. Mol. Sci.* 16 (2015) 23279–23299. <https://doi.org/10.3390/ijms161023279>.

[208] M. Chen, H. Yin, P. Bai, P. Miao, X. Deng, Y. Xu, J. Hu, J. Yin, ABC transporters affect the elimination and toxicity of CdTe quantum dots in liver and kidney cells, *Toxicol. Appl. Pharmacol.* 303 (2016) 11–20. <https://doi.org/10.1016/j.taap.2016.04.017>.

[209] L. Paesano, A. Perotti, A. Buschini, C. Carubbi, M. Marmiroli, E. Maestri, S. Iannotta, N. Marmiroli, Markers for toxicity to HepG2 exposed to cadmium sulphide quantum dots; damage to mitochondria, *Toxicology*. 374 (2016) 18–28. <https://doi.org/10.1016/j.tox.2016.11.012>.

[210] K. Shivaji, S. Mani, P. Ponmurugan, C.S. De Castro, M. Lloyd Davies, M.G. Balasubramanian, S. Pitchaimuthu, Green-synthesis-derived CdS quantum dots using tea leaf extract: Antimicrobial, bioimaging, and therapeutic applications in lung cancer cells, *ACS Appl. Nano Mater.* 1 (2018) 1683–1693. <https://doi.org/10.1021/acsanm.8b00147>.

[211] S. Bratskaya, K. Sergeeva, M. Kononova, E. Modin, E. Svirshchevskaya, A. Sergeev, A. Mironenko, A. Pestov, Ligand-assisted synthesis and cytotoxicity of ZnSe quantum dots stabilized by N-(2-carboxyethyl) chitosans, *Colloids Surf. B Biointerfaces*. 182 (2019) 110342–110342. <https://doi.org/10.1016/j.colsurfb.2019.06.071>.

[212] X. Wang, W. Dai, X. Li, Z. Chen, Z. Zheng, Z. Chen, G. Zhang, L. Xiong, S. Duo, Effects of L-cysteine on

- the photoluminescence, electronic and cytotoxicity properties of ZnS:O quantum dots, *J. Alloys Compd.* 825 (2020) 154052–15410. <https://doi.org/10.1016/j.jallcom.2020.154052>.
- [213] M.L. Desai, S. Jha, H. Basu, S. Saha, R.K. Singhal, S.K. Kailasa, Simple hydrothermal approach for synthesis of fluorescent molybdenum disulfide quantum dots: Sensing of Cr³⁺ ion and cellular imaging, *Mater. Sci. Eng. C.* 111 (2020) 110778–111087. <https://doi.org/10.1016/j.msec.2020.110778>.
- [214] V. Arul, T. Nesakumar, J. Immanuel, Y. Rok, M. Gopalakrishnan, Biological and catalytic applications of green synthesized fluorescent N-doped carbon dots using *Hylocereus undatus*, *J. Photochem. Photobiol. B Biol.* 168 (2017) 142–148. <https://doi.org/10.1016/j.jphotobiol.2017.02.007>.
- [215] S.L. D'souza, B. Deshmukh, J.R. Bhamore, K.A. Rawat, N. Lenka, S.K. Kailasa, Synthesis of fluorescent nitrogen-doped carbon dots from dried shrimps for cell imaging and boldine drug delivery system, *RSC Adv.* 6 (2016) 12169–12179. <https://doi.org/10.1039/C5RA24621K>.
- [216] S.M. de Carvalho, Z.I.P. Lobato, M.I.M.C. Guedes, M.F. Leite, A.A.P. Mansur, H.S. Mansur, In vitro and in vivo assessment of nanotoxicity of CdS quantum dot/aminopolysaccharide bionanoconjugates, *Mater. Sci. Eng. C.* 71 (2016) 412–424. <https://doi.org/10.1016/j.msec.2016.10.023>.
- [217] X. Li, X. Yang, L. Yuwen, W. Yang, L. Weng, Z. Teng, L. Wang, Evaluation of toxic effects of CdTe quantum dots on the reproductive system in adult male mice, *Biomaterials.* 96 (2016) 24–32. <https://doi.org/10.1016/j.biomaterials.2016.04.014>.
- [218] V. Zalgevicene, V. Kulvietis, D. Bulotiene, E. Zurauskas, A. Laurinaviciene, A. Skripka, R. Rotomskis, Quantum dots mediated embryotoxicity via placental damage, *Reprod. Toxicol.* 73 (2017) 222–231. <https://doi.org/10.1016/j.reprotox.2017.08.016>.
- [219] S.J. Rosenthal, J.C. Chang, O. Kovtun, J.R. McBride, I.D. Tomlinson, Biocompatible quantum dots for biological applications, *Chem. Biol.* 18 (2011) 10–24. <https://doi.org/10.1016/j.chembiol.2010.11.013>.
- [220] H. Moon, C. Lee, W. Lee, J. Kim, H. Chae, Stability of quantum dots, quantum dot films, and quantum dot light-emitting diodes for display applications, *Adv. Mater.* 31 (2019) 1–14. <https://doi.org/10.1002/adma.201804294>.
- [221] D. Dupont, M.D. Tessier, P.F. Smet, Z. Hens, Indium phosphide-based quantum dots with shell-enhanced absorption for luminescent down-conversion, *Adv. Mater.* 29 (2017) 1700686–1700692. <https://doi.org/10.1002/adma.201700686>
- [222] H.C. Wang, H. Zhang, H.Y. Chen, H.C. Yeh, M.R. Tseng, R.J. Chung, S. Chen, R.S. Liu, Cadmium-free InP/ZnSeS/ZnS heterostructure-based quantum dot light-emitting diodes with a ZnMgO electron transport layer and a brightness of over 10000 cd m⁻², *Small.* 13 (2017) 1603962–1603969. <https://doi.org/10.1002/sml.201603962>.
- [223] S. Kim, T. Kim, M. Kang, S.K. Kwak, T.W. Yoo, L.S. Park, I. Yang, S. Hwang, J.E. Lee, S.K. Kim, S.W. Kim, Highly luminescent InP/GaP/ZnS nanocrystals and their application to white light-emitting diodes, *J. Am. Chem. Soc.* 134 (2012) 3804–3809. <https://doi.org/10.1021/ja210211z>.
- [224] T. Kim, S.W. Kim, M. Kang, S.-W. Kim, Large-scale synthesis of InPZnS alloy quantum dots with dodecanethiol as a composition controller, *J. Phys. Chem. Lett.* 3 (2012) 214–218.

1547 <https://doi.org/10.1021/jz201605d>.

1548 [225] Y. Fu, M.-S. Jang, T. Wu, J.H. Lee, Y. Li, D.S. Lee, H.Y. Yang, Multifunctional hyaluronic acid-mediated

1549 quantum dots for targeted intracellular protein delivery and real-time fluorescence imaging, *Carbohydr.*

1550 *Polym.* 224 (2019) 115174–115183. <https://doi.org/10.1016/j.carbpol.2019.115174>.

1551 [226] S.-Y. Park, H.-S. Kim, J. Yoo, S. Kwon, T.J. Shin, K. Kim, S. Jeong, Y.-S. Seo, Long-term stability of

1552 CdSe/CdZnS quantum dot encapsulated in a multi-lamellar microcapsule, *Nanotechnology* 26 (2015)

1553 275602–275611. <http://dx.doi.org/10.1088/0957-4484/26/27/275602>.

1554